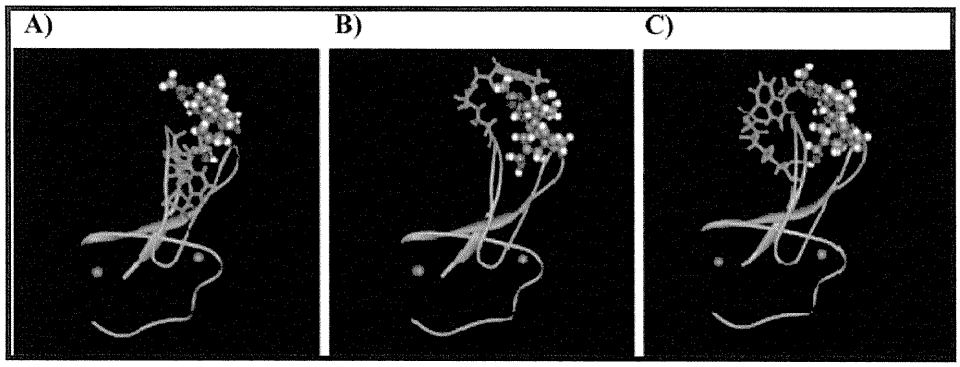

Figure 1. Structural models of dansyl-labeled δC1b analogues. (A) Y238K(DnsG), (B) S240K(DnsG), and (C) T242K(DnsG). Space-filling models indicate phorbol esters and zinc atoms.

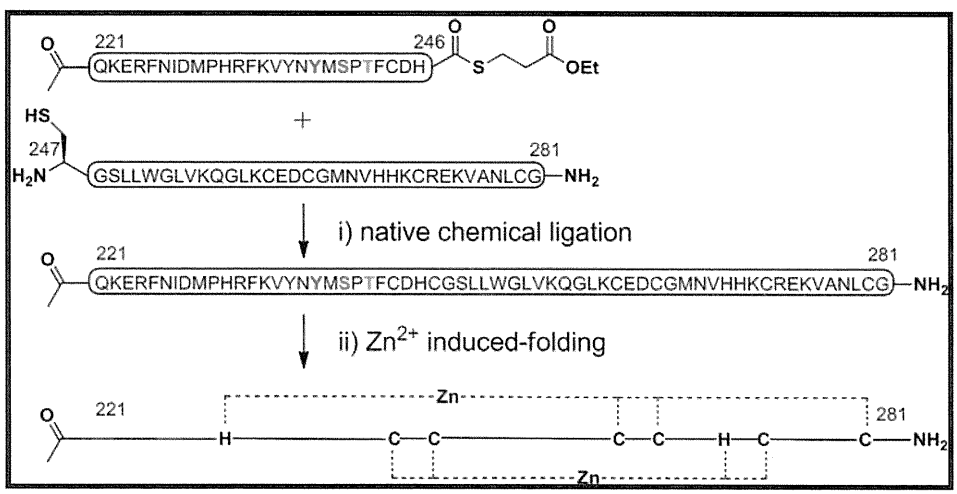

Figure 2. Schematic representation of construction of dansyl-labaled δC1b. (i) 100 mM phosphate buffer (pH 8.5), 6 M Gn·HCl, 2 mM EDTA, TCEP·HCl, thiophenol, N_2, 37 °C; (ii) 50 mM Tris·HCl (pH 7.4), 150 mM NaCl, 1 mM DTT, 0.1 mM $ZnCl_2$, 4 °C.

dansyl-labeled δC1b domain analogues, a native chemical ligation (NCL) method was adopted (*18, 24*). Three N-terminal peptide fragments (dansyl-labeled δC1b(221−246)) and a common C-terminal peptide fragment (δC1b(247−281)) were separately synthesized. A purified δC1b(247−281) and three dansyl-labeled δC1b(221−246) fragments were condensed by an NCL method (Figure 2). The ligation reaction was performed with 0.8 mM of each peptide fragment in 100 mM phosphate buffer (pH 8.5) containing 6 M Gn·HCl, 2 mM EDTA, and 3% thiophenol at 37 °C. The progress of the ligation reaction was monitored by HPLC (Supporting Information). The condensed δC1b domains were identified by ESI-TOF-mass spectra (Supporting Information Table S1). The purified peptides were lyophilized and obtained as powders. Total yields of NCL were 38% for Y238K(DnsG), 48% for S240K(DnsG), and 41% for T242K(DnsG). Folding of the synthetic δC1b domain was performed by dialysis against Zn^{2+} containing buffer (50 mM Tris·HCl (pH 7.4), 150 mM NaCl, 1 mM DTT, 0.1 mM $ZnCl_2$) at 4 °C.

Characterization of Synthetic δC1b Analogues. The apparent [^{3}H]PDBu binding affinity of the dansyl-labeled δC1b domains was evaluated by the method described previously (*18, 19*). S240K(DnsG) and T242K(DnsG) showed K_d values comparable to that of the wild type. However, B_{max} values were 6% for S240K(DnsG) and 11% for T242K(DnsG) compared to the wild type (Table 1). The results indicate that dansyl-labeling might partly impair the efficiency of correct folding of the synthetic δC1b domain. Y238K(DnsG) did not possess significant binding affinity for PDBu, consistent with the predictions from the modeling. We conclude that the dansyl-labeled δC1b domains maintain potent binding activity and correct folding, at least for an appreciable proportion of the product, in those cases in which the dansyl group is located outside the binding pocket.

Table 1. Binding Activity of the Synthetic δC1b Analogues to [^{3}H]PDBu

peptides	K_d (nM)[a]	B_{max} (pmol/mg)[b]
wild type	0.34 ± 0.08	38000
Y238K(DnsG)	n.d.[c]	11
S240K(DnsG)	0.18 ± 0.05	2100
T242K(DnsG)	0.35 ± 0.04	3700

[a] Dissociation constant for the synthetic δC1b binding to [^{3}H]PDBu. Mean ± SEM. [b] Numbers of binding sites. [c] Not determined.

To estimate the influence of dansyl-labeling on folding of δC1b domain, circular dichroism (CD) spectroscopy of S240K(DnsG) and T242K(DnsG) was performed for comparison before and after dialysis (Figure 3). Since the CD spectrum of the synthetic δC1b(231−281) is similar to that of the recombinant δC1b domain (*18*), Y238K(DnsG)-δC1b(231−281) was used to evaluate the effects of dansyl-labeling on folding of Y238K(DnsG) (Supporting Information Figure S3). The addition of $ZnCl_2$ did not cause a significant change of CD spectra of Y238K(DnsG)-δC1b(231−281). Thus, the introduction of a dansyl group into Tyr238 might interfere correct folding. The CD spectra of both of the dansyl-labeled δC1b domains before dialysis showed broad minima around 205 nm, suggesting random coil structures (*25*). CD spectra of the dialyzed dansyl-labeled δC1b domains exhibited decreases of negative cotton effects around 205 nm, which were similar to those of recombinant and synthetic δC1b domains (*18, 25*).

The apparent [^{3}H]PDBu binding affinities and CD spectra of the dansyl-labeled δC1b domains, S240K(DnsG) and

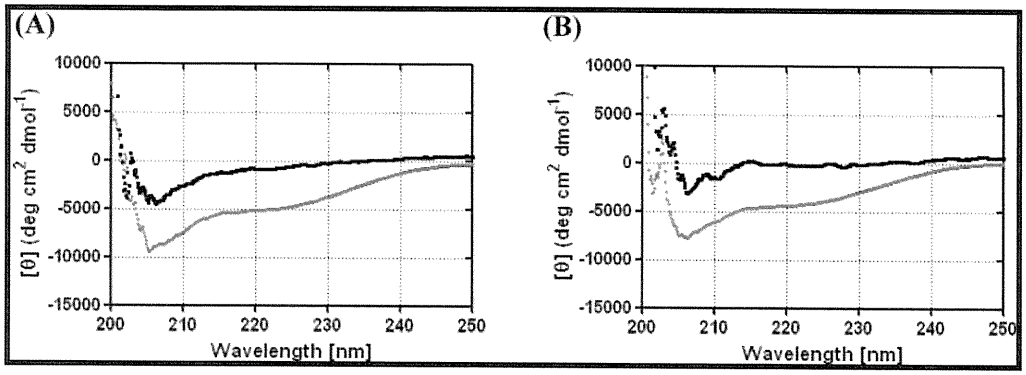

Figure 3. Changes of CD spectra of dansyl-labeled δC1b analogues, S240K(DnsG) (A) and T242K(DnsG) (B). Blue and black plots show profiles before and after dialysis against Zn^{2+} containing buffer, respectively.

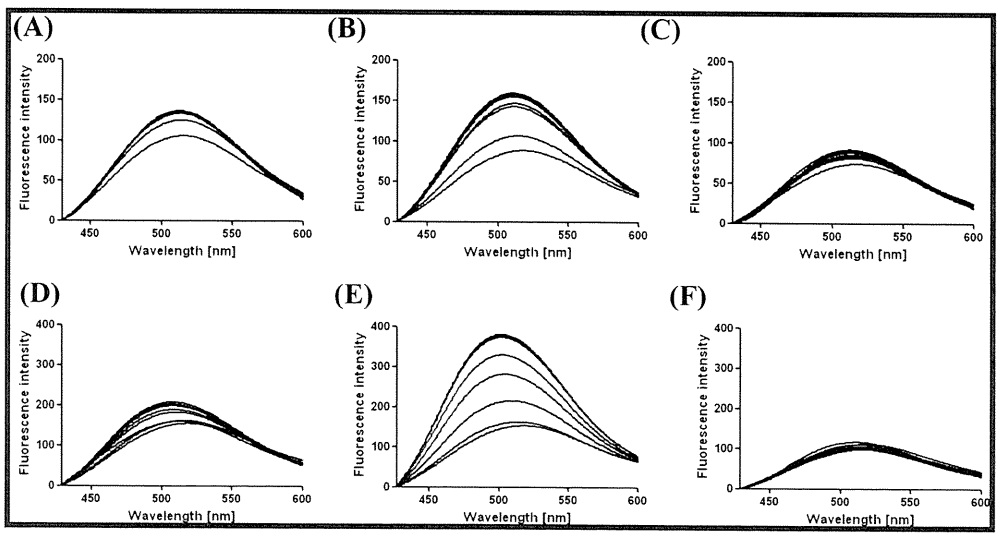

Figure 4. Fluorescent spectra obtained by ligand titration experiments for dansyl-labeled δC1b analogues. Panels A−C show titrations of PDBu, PMA, and PDA against S240K(DnsG), respectively. Panels D−F show titrations of PDBu, PMA, and PDA against T242K(DnsG), respectively. Dansyl-labeled δC1b analogue, 0.5 μM; buffer, 50 mM Tris·HCl (pH 7.4), 150 mM NaCl, 1 mM DTT, 0.1 mM $ZnCl_2$, 5 μg/mL phosphatidylserine; ligand, 0.02, 0.06, 0.1, 0.14, 0.18, 0.22, 0.26, 0.3 equiv, λ_{ex} = 330 nm.

T242K(DnsG), demonstrated that insertion of dansyl groups at Ser 240 and at Thr 242 maintained correct folding and strong ligand binding affinity comparable to that of the wild type, although involving reduction of the stability of the domains.

Titration of Ligands to Fluorescent-Labeled δC1b Domain Analogues. To evaluate the fluorescent properties of dansyl-labeled δC1b domain, fluorescent emission spectra were measured during ligand titration. As test ligands, the phorbol esters PDBu (K_i = 0.72 ± 0.06 nM), phorbol 12-myristate 13-acetate (PMA) (K_i = 0.14 ± 0.04 nM), and phorbol 12,13-diacetate (PDA) (K_i = 68.9 ± 5.9 nM), were employed. Values of K_i were determined by competitive binding assays using [^{3}H]PDBu (Supporting Information). Fluorescent titration experiments showed that the spectra of the dansyl-labeled δC1b domain analogues changed according to the ligand concentration. S240K(DnsG) showed 1.3-, 1.8-, and 1.2-fold increases in fluorescent intensity and blue shifts in the emission maxima upon additions of PDBu, PMA, and PDA, respectively (Figures 4A−C). T242K(DnsG) showed 1.3-, 2.6-, and 1.1-fold increases in fluorescent intensity and blue shifts in the emission maxima upon additions of PDBu, PMA, and PDA, respectively (Figures 4D−F). The rank order of increases in fluorescent intensity upon addition of the above ligands to S240K(DnsG) and T242K(DnsG) thus corresponded to that of their K_i values.

Since dansyl-Gly showed stronger fluorescent intensity in a hydrophobic environment than in a hydrophilic environment (Supporting Information Figure S1), the increases in fluorescence intensity upon ligand titration of S240K(DnsG) and T242K(DnsG) suggested that the environment surrounding the dansyl moiety was changed to become more hydrophobic upon ligand binding (*26–28*). As predicted in the modeling study, the dansyl group was not located in the binding pocket, preventing binding. Even after ligand binding, the dansyl group will still be located outside the binding pocket. Thus, the binding of ligands to the binding pocket must make the environment surrounding the dansyl more hydrophobic, possibly due to interactions between dansyl and the long alkyl chains of the ligands. In addition, T242K(DnsG) showed stronger fluorescence intensity than did S240K(DnsG). This phenomenon corresponds to their relative B_{max} values observed in the [^{3}H]PDBu binding assay (Figures 1B, C, Table 1). A reason could be the hydrogen bonding network at the binding site of phorbol ester on the δC1b domain. The C20 hydroxy group of the phorbol ester accepts a hydrogen bond from the main-chain NH of T242 (*20*). Thus, the stronger fluorescent intensity of T242K(DnsG) could be due to a closer distance to the bound ligand. Furthermore, saturation of the increase in fluorescent intensity was observed when the ligand concentration reached 0.05−0.1 μM (10−20% of the peptide concentration) (Figure 5). This result is consistent with the B_{max} values of dansyl-labeled δC1b: 6−11% of the wild type. The K_d values based on titration of ligands to the dansyl-labeled δC1b domains were evaluated (Table 2). As a control experiment, S240K(DnsG) dialyzed without Zn^{2+} did not

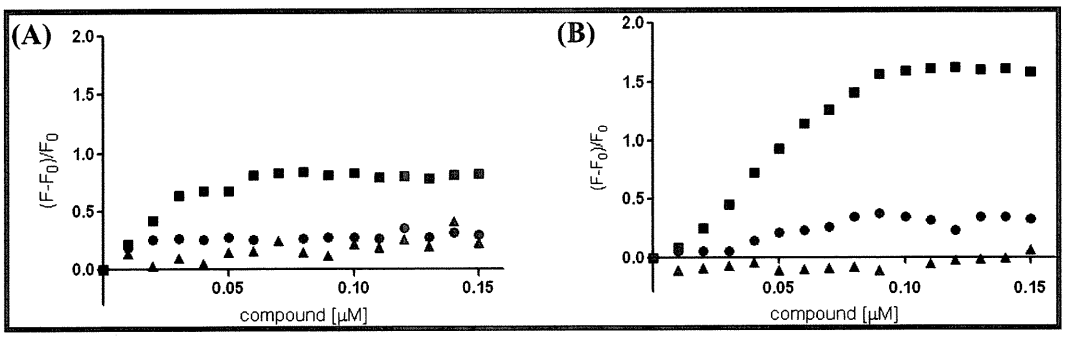

Figure 5. Plots of change of fluorescence intensity from titration experiments using S240K(DnsG) (A) and T242K(DnsG) (B). Dansyl-labeled δC1b analogue, 0.5 μM; square, PMA; round, PDBu; triangle, PDA.

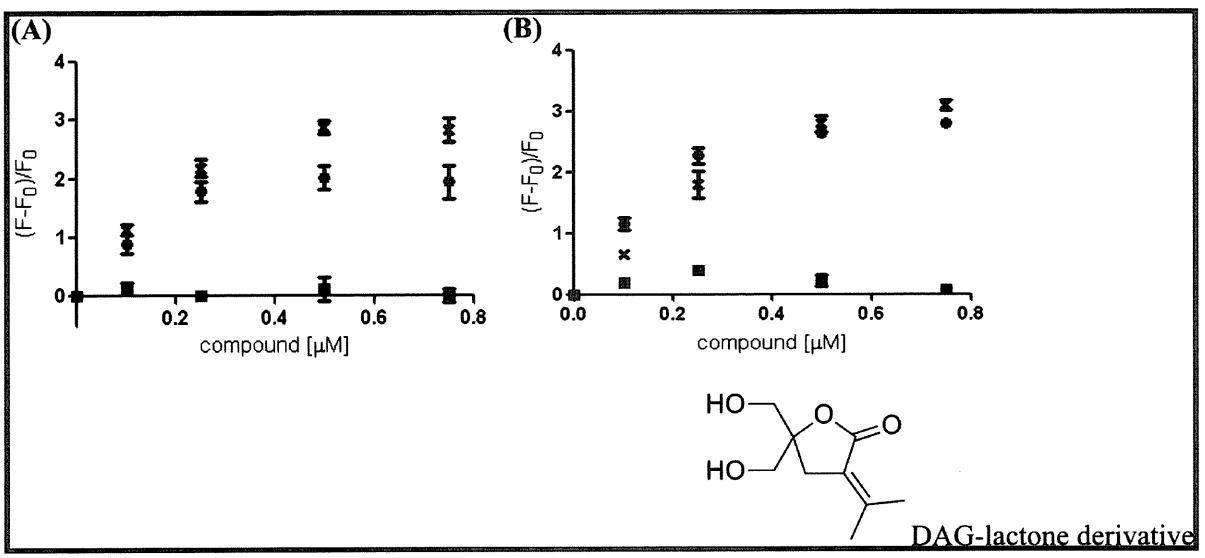

Figure 6. Plots of change of fluorescence intensity from 96-well plates-based titration experiments of S240K(DnsG) (A) and T242K(DnsG) (B). cross, PMA; circle, PDBu; square, DAG-lactone derivative.

Table 2. K_d Values of the Fluorescent-Labeled δC1b Domain Analogues Based on Titration of Ligands

compound	S240K(DnsG) K_d (nM)[a]	T242K(DnsG) K_d (nM)[a]
PMA	20.6	121.6
PDBu	5.83	110
PDA	Not convergent	Not fitting

[a] Dissociation constant for the fluorescent-labeled δC1b domain analogues to each compound was calculated.

show any significant increase in fluorescent intensity upon the addition of PDBu (Supporting Information Figure S2), suggesting that correct folding involving zinc-finger formation is critical for ligand binding. The detection limit might be the level of the fluorescent intensity of PDA. The results of titration experiments indicate that, upon ligand binding to correctly folded C1b domains, the site surrounding the ligand binding pocket becomes more hydrophobic. Even if some uncertainty remains about the relative contributions of the mechanisms leading to this change in hydrophobicity, the core finding is that ligand binding was detected by an increase in fluorescent intensity, which corresponds to binding affinity. The binding activity of ligands can be possibly evaluated by increases in fluorescent intensity upon the consideration of LogP values.

S240K(DnsG) and T242K(DnsG) were employed in fluorescent experiments utilizing 96-well plates for initial assessment of their suitability to high-throughput screening. Plots of changes of fluorescent intensity against the ligand concentration showed dose-dependent curves similar to those in titration experiments (Figure 6). The results indicate that the present fluorescent-responsive C1b domains can be used for screening of novel PKC pharmacophores.

CONCLUSIONS

In this study, three kinds of dansyl-labeled δC1b domains, Y238K(DnsG), S240K(DnsG), and T242K(DnsG), were synthetically constructed in an efficient way by utilizing Fmoc-SPPS and an NCL method. The results of CD measurements and [^{3}H]PDBu binding assays indicated that the position of dansyl-labeling was critical for maintenance of native functions including proper folding. The ligand titration of dansyl-labeled δC1b showed that the change of fluorescent spectra corresponded to the K_i values of the ligands. Furthermore, S240K(DnsG) and T242K(DnsG) were utilized for measurements using a 96-well plate-based format, indicating that evaluation of ligand binding could be performed in a high-throughput fashion. The present fluorescent-responsive domains were successfully utilized in vitro. However, through optimization of the stability of the fluorescent-labeled δC1b domain, these domains might also be adapted for cell-based assays as efficient DAG sensors.

ACKNOWLEDGMENT

The authors thank Professor Kazunari Akiyoshi (Graduate School of Engineering, Kyoto University) for assistance in the CD experiments. This study was supported in part by the Naito Foundation for Science (to W. N.) and in part by the Intramural Research Program of the NIH, Center for Cancer Research, National Cancer Institute. N. O. is supported by the Japan Society for Promotion of Science.

Supporting Information Available: Detailed materials and methods. This material is available free of charge via the Internet at http://pubs.acs.org.

LITERATURE CITED

(1) Nishizuka, Y. (1992) Intracellular signaling by hydrolysis of phospholipids and activation of protein kinase C. *Science 258*, 607–614.

(2) Newton, A. C. (1995) Protein kinase C: structure, function, and regulation. *J. Biol. Chem. 270*, 28495–28498.

(3) Watanabe, T., Ono, Y., Taniyama, Y., Hazama, K., Igarashi, K., Ogita, K., Kikkawa, U., and Nishizuka, Y. (1992) Cell division arrest induced by phorbol ester in CHO cells overexpressing protein kinase C-delta subspecies. *Proc. Natl. Acad. Sci. U.S.A. 89*, 10159–10163.

(4) Mischak, H., Pierce, J. H., Goodnight, J., Kazanietz, M. G., Blumberg, P. M., and Mushinski, J. F. (1993) Phorbol ester-induced myeloid differentiation is mediated by protein kinase C-alpha and -delta and not by protein kinase C-beta II, -epsilon, -zeta, and -eta. *J. Biol. Chem. 268*, 20110–20115.

(5) Li, C., Wernig, E., Leitges, M., Hu, Y., and Xu, Q. (2003) Mechanical stress-activated PKCdelta regulates smooth muscle cell migration. *FASEB J. 17*, 2106–2108.

(6) Ghayur, T., Hugunin, M., Talanian, R. V., Ratnofsky, S., Quinlan, C., Emoto, Y., Pandey, P., Datta, R., Huang, Y., Kharbanda, S., Allen, H., Kamen, R., Wong, W., and Kufe, D. (1996) Proteolytic activation of protein kinase C delta by an ICE/CED 3-like protease induces characteristics of apoptosis. *J. Exp. Med. 184*, 2399–2404.

(7) Humphries, M. J., Limesand, K. H., Schneider, J. C., Nakayama, K. I., Anderson, S. M., and Reyland, M. E. (2006) Suppression of apoptosis in the protein kinase Cdelta null mouse in vivo. *J. Biol. Chem. 281*, 9728–9737.

(8) Alkon, D. L., Sun, M. K., and Nelson, T. J. (2007) PKC signaling deficits: a mechanistic hypothesis for the origins of Alzheimer's disease. *Trends Pharmacol. Sci. 28*, 51–60.

(9) Churchill, E., Budas, G., Vallentin, A., Koyanagi, T., and Mochly-Rosen, D. (2008) PKC isozymes in chronic cardiac disease: possible therapeutic targets? *Annu. Rev. Pharmacol. Toxicol. 48*, 569–599.

(10) O'Brian, C. A., Ward, N. E., Stewart, J. R., Chu, F., Mackay, H. J., and Twelves, C. (2001) Prospects for targeting protein kinase C isozymes in the therapy of drug-resistant cancer—an evolving story. *Cancer Metastasis Rev. 20*, 95–100.

(11) Tamamura, H., Sigano, D. M., Lewin, N. E., Blumberg, P. M., and Marquez, V. E. (2004) Conformationally constrained analogues of diacylglycerol. 20. The search for an elusive binding site on protein kinase C through relocation of the carbonyl pharmacophore along the sn-1 side chain of 1,2-diacylglycerol lactones. *J. Med. Chem. 47*, 644–655.

(12) Tamamura, H., Sigano, D. M., Lewin, N. E., Peach, M. L., Nicklaus, M. C., Blumberg, P. M., and Marquez, V. E. (2004) Conformationally constrained analogues of diacylglycerol (DAG). 23. Hydrophobic ligand-protein interactions versus ligand-lipid interactions of DAG-lactones with protein kinase C (PK-C). *J. Med. Chem. 47*, 4858–4864.

(13) Marquez, V. E., and Blumberg, P. M. (2003) Synthetic diacylglycerols (DAG) and DAG-lactones as activators of protein kinase C (PK-C). *Acc. Chem. Res. 36*, 434–443.

(14) Morii, T., Sugimoto, K., Makino, K., Otsuka, M., Imoto, K., and Mori, Y. (2002) A new fluorescent biosensor for inositol trisphosphate. *J. Am. Chem. Soc. 7*, 1138–1139.

(15) Venkatraman, P., Nguyen, T. T., Sainlos, M., Bilsel, O., Chitta, S., Imperiali, B., and Stern, L. J. (2007) Fluorogenic probes for monitoring peptide binding to class II MHC proteins in living cells. *Nat. Chem. Biol. 3*, 201–202.

(16) Joshi, B. P., and Lee, K. H. (2008) Synthesis of highly selective fluorescent peptide probes for metal ions: tuning selective metal monitoring with secondary structure. *Bioorg. Med. Chem. 16*, 8501–8509.

(17) Simard, J. R., Grütter, C., Pawar, V., Aust, B., Wolf, A., Rabiller, M., Wulfert, S., Robubi, A., Klüter, S., Ottmann, C., and Rauh, D. (2009) High-throughput screening to Identify inhibitors which stabilize inactive kinase conformations in p38α. *J. Am. Chem. Soc. 131*, 18478–18488.

(18) Ohashi, N., Nomura, W., Kato, M., Narumi, T., Lewin, N. E., Blumberg, P. M., and Tamamura, H. (2009) Synthesis of protein kinase Cδ C1b domain by native chemical ligation methodology and characterization of its folding and ligand binding. *J. Pept. Sci. 10*, 642–646.

(19) Kazanietz, M. G., Areces, L. B., Bahador, A., Mischak, H., Goodnight, J., Mushinski, J. F., and Blumberg, P. M. (1993) Characterization of ligand and substrate specificity for the calcium-dependent and calcium-independent protein kinase C isozymes. *Mol. Pharmacol. 44*, 298–307.

(20) Zhang, G., Kazanietz, M. G., Blumberg, P. M., and Hurley, J. H. (1995) Crystal structure of the cys2 activator-binding domain of protein kinase C delta in complex with phorbol ester. *Cell 81*, 917–924.

(21) Kazanietz, M. G., Wang, S., Milne, G. W., Lewin, N. E., Liu, H. L., and Blumberg, P. M. (1995) Residues in the second cysteine-rich region of protein kinase C delta relevant to phorbol ester binding as revealed by site-directed mutagenesis. *J. Biol. Chem. 270*, 21852–21859.

(22) Soini, E., and Hemmila, I. (1979) Fluoroimmunoassay: present status and key problems. *Clin. Chem. 25*, 353–361.

(23) Irie, K., Oie, K., Nakahara, A., Yanai, Y., Ohigashi, H., Wender, P. A., Fukuda, H., Konishi, H., and Kikkawa, U. (1998) Molecular basis for protein kinase C isozyme-selective binding: the synthesis, folding, and phorbol ester binding of the cysteine-rich domains of all protein kinase C isozymes. *J. Am. Chem. Soc. 120*, 9159–9167.

(24) Dawson, P. E., Churchill, M. J., Ghadiri, M. R., and Kent, S. B. H. (1997) Chemical protein synthesis by solid phase ligation of unprotected peptide segments. *J. Am. Chem. Soc. 119*, 4325–4329.

(25) Zimenkov, Y., Dublin, S. N., Ni, R., Tu, R. S., Breedveld, V., Apkarian, R. P., and Conticell, V. P. (2006) Rational design of a reversible pH-responsive switch for peptide self-assembly. *J. Am. Chem. Soc. 128*, 6770–6771.

(26) Ikeda, H., Nakamura, M., Ise, N., Oguma, N., Nakamura, A., Ikeda, T., Toda, F., and Ueno, A. (1996) Fluorescent cyclodextrins for molecule sensing: fluorescent properties, NMR characterization, and inclusion phenomena of n-dansylleucine-modified cyclodextrins. *J. Am. Chem. Soc. 118*, 10980–10988.

(27) Ikunaga, T., Ikeda, H., and Ueno, A. (1999) The effects of avidin on inclusion phenomena and fluorescent properties of biotin-appended dansyl-modified β-cyclodextrin. *Chem.—Eur. J. 5*, 2698–2704.

(28) Matsumura, S., Sakamoto, S., Ueno, A., and Mihara, H. (2000) Construction of α-helix peptides with β-cyclodextrin and dansyl units and their conformational and molecular sensing properties. *Chem.—Eur. J. 6*, 1781–1788.

BC100414A

CHEMMEDCHEM

DOI: 10.1002/cmdc.201000548

Azamacrocyclic Metal Complexes as CXCR4 Antagonists

Tomohiro Tanaka,[a] Tetsuo Narumi,*[a] Taro Ozaki,[a] Akira Sohma,[a] Nami Ohashi,[a] Chie Hashimoto,[a] Kyoko Itotani,[a] Wataru Nomura,[a] Tsutomu Murakami,[b] Naoki Yamamoto,[b, c] and Hirokazu Tamamura*[a]

The chemokine receptor CXCR4 is a member of the seven transmembrane GPCR family, which is implicated in multiple diseases, including HIV infection, cancers, and rheumatoid arthritis. Low-molecular-weight nonpeptidic compounds, including AMD3100 and various pyridyl macrocyclic zinc(II) complexes, have been identified as selective antagonists of CXCR4. In the present study, structure–activity relationship studies were performed by combining the common structural features of alkylamino and pyridiyl macrocyclic antagonists. Several new zinc(II) or copper(II) complexes demonstrated potent anti-HIV activity, strong CXCR4-binding activity, and significant inhibitory activity against Ca^{2+} mobilization induced by CXCL12 stimulation. These results may prove useful in the design of novel CXCR4 antagonists, and the compounds described could potentially be developed as therapeutics against CXCR4-relevant diseases or chemical probes to study the biological activity of CXCR4.

Introduction

The chemokine receptor CXCR4, which transduces signals of its endogenous ligand, CXCL12/stromal cell-derived factor-1 (SDF-1),[1–4] is classified as a member of the seven transmembrane GPCR family, and plays a physiological role via its interaction with CXCL12 in chemotaxis,[5] angiogenesis,[6,7] and neurogenesis[8,9] in embryonic stages. CXCR4 is, however, relevant to multiple diseases including HIV infection/AIDS,[10,11] metastasis of several types of cancer,[12–14] leukemia cell progression,[15,16] and rheumatoid arthritis (RA),[17,18] and is considered an attractive drug target to combat these diseases. Thus, inhibitors targeting CXCR4 are expected to be useful for drug discovery.

Several CXCR4 antagonists have been reported,[19–35] including our discovery of the highly potent CXCR4 antagonist T140, a 14-mer peptide with a disulfide bridge, its smaller derivative, the 5-mer cyclic peptide FC131, and several other potent analogues.[19,24–26,28–30] Clinical development of these peptidic antagonists could be pursued using specific administration strategies involving biodegradable microcapsules.[14,36] However, herein we focus on novel nonpeptidic low-molecular-weight CXCR4 antagonists. To date, AMD3100 (**1**),[20,22] Dpa-Zn complex (**2**),[37] KRH-1636,[27] and other compounds[31–35] have been developed in this and other laboratories as low-molecular-weight nonpeptidic CXCR4 antagonists. The present study reports structure–activity relationship studies based on the combination of common structural motifs, such as xylene scaffolds and cationic moieties that are present in the aforementioned compounds.

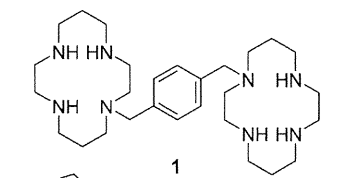

1

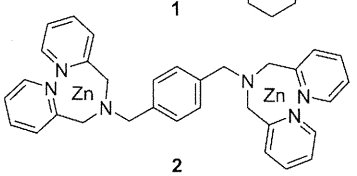

2

Results and Discussion

In order to determine spatially suitable positioning of cationic moieties, *p*- and *m*-xylenes were utilized as spacers. Cationic moieties such as bis(pyridin-2-ylmethyl)amine (dipicolylamine), 1,4,7,10-tetraazacyclododecane (cyclen), and 1,4,8,11-tetraazacyclotetradecane (cyclam) were introduced as R^1 and R^2 (Figure 1). This combination of R^1, R^2, and spacer groups led to the design and synthesis of compounds **12**–**31**.

The CXCR4 binding activity of synthetic compounds was assessed based on the inhibition of [^{125}I]CXCL12 binding to Jurkat cells, which express CXCR4.[38] The percent inhibition of all compounds at 1 μM is shown in Table 1. Seven compounds (**16**, **17**, **20**–**22**, **28**, and **29**, Table 1) resulted in greater than 87% inhibition. The high activity of **16** is consistent with re-

[a] *T. Tanaka, Dr. T. Narumi, T. Ozaki, A. Sohma, N. Ohashi, C. Hashimoto, K. Itotani, Dr. W. Nomura, Prof. H. Tamamura*
Institute of Biomaterials and Bioengineering
Tokyo Medical and Dental University
2-3-10 Kandasurugadai, Chiyoda-ku, Tokyo 101-0062 (Japan)
Fax: (+81) 3-5280-8039
E-mail: tamamura.mr@tmd.ac.jp

[b] *Dr. T. Murakami, Prof. N. Yamamoto*
AIDS Research Center, National Institute of Infectious Diseases
1-23-1 Toyama, Shinjuku-ku, Tokyo 162-8640 (Japan)

[c] *Prof. N. Yamamoto*
Department of Microbiology, Yong Loo Lin School of Medicine
National University of Singapore, Singapore 117597 (Singapore)

Supporting information for this article is available on the WWW under http://dx.doi.org/10.1002/cmdc.201000548.

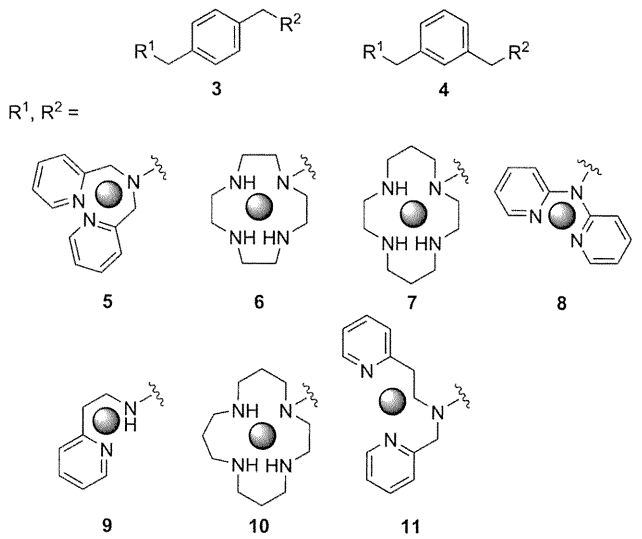

Figure 1. The structures of aromatic spacers (upper) and cationic moieties (R^1 and R^2). The shaded circle represents the position of the metal cation (Zn^{II} or Cu^{II}) in the chelate.

sults reported previously.[20,22] The anti-HIV activities of **17** and **29**, which contain only cyclam or cyclal rings, were reported by De Clercq et al.[39,40] Compounds with only pyridine and/or cyclen rings did not show any high binding activity. The presence of azamacrocyclic rings is presumably indispensable to the interaction of these compounds with CXCR4, and the size of rings appears to be important because not only compounds **16** and **17**, with two cyclam rings in the molecule, but also compounds **28** and **29**, with two cyclal rings, have remarkably more potent CXCR4 binding activity than compounds **14** and **15**, which have two cyclen rings. Compound **22**, with a *p*-xylene moiety, exhibited higher activity than compound **23**, which has an *m*-xylene moiety, indicating that *p*-xylene is more suitable than *m*-xylene as a spacer for approximate positioning of cationic moieties. At 0.1 μM, compound **22** resulted in 86% inhibition of [^{125}I]CXCL12 binding, while the other six compounds exhibited 37–66% inhibition. The IC_{50} value of compound **22** was estimated to be 37 nM.

$ZnCl_2$ was added to phosphate-buffered saline (PBS) solutions of these 20 compounds, **12–31**, to form zinc(II) complexes. The percent inhibition for each compound at 1 μM against [^{125}I]CXCL12 binding was determined and is given in Table 1. Zinc complexation of **12–15**, **18**, **19**, and **23** resulted in a remarkable increase in CXCR4 binding activity compared to the corresponding zinc-free compounds. These molecules contain dipicolylamine and/or cyclen moieties, suggesting that chelation of the nitrogen atoms with the zinc(II) ion significantly affects their interactions with CXCR4. The high activity of the zinc chelates of **12** and **13** is consistent with results provided in our previous paper.[37] Additionally, the anti-HIV activity of zinc complexes of **14** and **15** was reported by Kimura et al.[41] For compounds with only dipicolylamine and/or cyclen macrocycles as cationic moieties (**12–15**, **18**, and **19**), zinc complexation is critical to achieve high binding activity; the corresponding zinc-free compounds exhibit no significant activity. Compounds **16**, **17**, **20–22**, **28**, and **29** demonstrated high binding affinity in metal-free states as well as in zinc complexation states, indicating that zinc complexation of either of the macrocyclic rings in these compounds is not essential for high activity. The CXCR4 binding activity and anti-HIV activity of the zinc complex of **16** were reported previously.[42,43] Measured inhibition percentages for 0.1 μM of the zinc complexes of **12**, **14–23**, **28**, and **29** are given in Table 1. The zinc complexes of **20–22**, **28**, and **29** at 0.1 μM exhibited greater than 79% inhibition of [^{125}I]CXCL12 binding, and the other eight zinc complexes (of **12**, **14–19**, and **23**,) showed less than 55% inhibition. The IC_{50} values of zinc complexes of **20–22**, **28**, and **29** were estimated to be 11, 8.3, 22, 40, and 52 nM, respectively. Zinc complexes of compounds containing a combination of cyclen and cyclam moieties, **20** and **21**, had remarkably potent IC_{50} values.

To form chelates with a copper(II) cation, $CuCl_2$ was added to solutions in PBS of **12-31**. The inhibition percentages of all the compounds at 1 μM against [^{125}I]CXCL12 binding are shown in Table 1. Copper complexes of **14** and **15** exhibited a significant increase in CXCR4 binding activity as compared to the corresponding copper-free compounds, a phenomenon which is also seen in the zinc chelates. These compounds have two cyclen moieties in the molecules, suggesting that zinc or copper complexation is critical for high binding activity. Compounds **16**, **17**, and **20–22** showed high binding affinities in metal-free states and zinc- and copper-complexed states, indicating that metallic complexation of the cyclam rings in these compounds is not necessary for high activity. The CXCR4 binding activity of the copper complex of **16** was previously reported.[42] For compounds **17**, **22**, **23**, **28**, and **29**, copper complexation caused a significant decrease in binding activity compared to the corresponding copper-free compounds, whereas for compounds **14**, **15**, **18**, and **19**, copper complexation caused an increase in binding activity. This phenomenon may be due to the difference in ring sizes and structures of macrocycles, and was not observed upon zinc-complex formation. Inhibition at 0.1 μM of the copper complexes of **16** and **20–22**, which exhibited greater than 85% inhibition of [^{125}I]CXCL12 binding at 1 μM, are given in Table 1. The copper complexes of **16**, **20**, **21**, and **22** at 0.1 μM showed 39, 69, 88, and 39% inhibition, respectively, with the IC_{50} value of the copper complex of **21** estimated to be 16 nM.

Molecular modeling analysis of compound **21** and its zinc(II) and copper(II) complexes predicted that these complexes would form a stable coordinate conformation as shown in Figure 2. In general, zinc(II) complexes are predicted to adopt a tetrahedral conformation, while copper(II) complexes form a planar four coordinate/square conformation. The zinc(II) complex of **21** is predicted to have a tetrahedral conformation and the copper(II) complex a square planar conformation in both the cyclen and cyclam rings. The carboxyl group of either Asp 171 or Asp 262 in CXCR4 is thought to coordinate strongly with zinc ions but not copper ions in the complexes,[41–43] and as a consequence, the zinc complex of **21** would bind more strongly than **21** or its copper complex. This order of binding

Table 1. CXCR4 binding activity of compounds **12–31** in the metal ion-free form, the zinc complex, and the copper complex.

Compd	Spacer	R^1	R^2	Metal free			Zinc complex			Copper complex		
				Inhibition[a] [%]		IC_{50}[b]	Inhibition[a] [%]		IC_{50}[b]	Inhibition[a] [%]		IC_{50}[b]
				1 μM	0.1 μM	[nM]	1 μM	0.1 μM	[nM]	1 μM	0.1 μM	[nM]
12	*p*-xylene	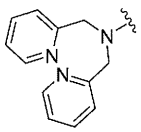	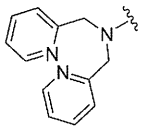	0	n.d.	n.d.	83±2	24±5	n.d.	10±4	n.d.	n.d.
13	*m*-xylene			0	n.d.	n.d.	31±3	n.d.	n.d.	0	n.d.	n.d.
14	*p*-xylene	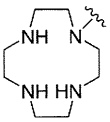	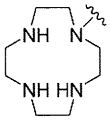	30±4	n.d.	n.d.	87±4	0	n.d.	60±2	n.d.	n.d.
15	*m*-xylene			33±2	n.d.	n.d.	94±1	13±6	n.d.	80±3	n.d.	n.d.
16	*p*-xylene	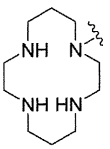	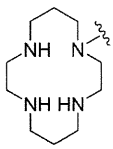	94±4	59±6	n.d.	97±5	28±3	n.d.	98±1	39±3	n.d.
17	*m*-xylene			95±3	49±9	n.d.	98±4	55±7	n.d.	75±1	n.d.	n.d.
18	*p*-xylene	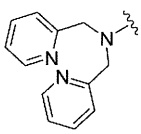	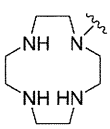	32±0.7	n.d.	n.d.	97±6	0	n.d.	52±3	n.d.	n.d.
19	*m*-xylene			17±5	n.d.	n.d.	91±4	0	n.d.	22±6	n.d.	n.d.
20	*p*-xylene	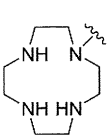	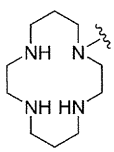	89±3	62±3	n.d.	>100	79±1	11	>100	69±3	n.d.
21	*m*-xylene			89±3	66±3	n.d.	92±3	>100	8.3	>100	88±1	16
22	*p*-xylene	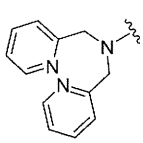	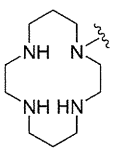	94±3	86±3	37	99±8	79±0.6	22	85±3	39±3	n.d.
23	*m*-xylene			58±8	n.d.	n.d.	90±17	37±0.3	n.d.	48±4	n.d.	n.d.
24	*p*-xylene	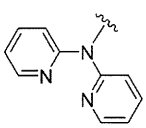	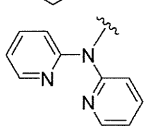	3±0.9	n.d.	n.d.	0	n.d.	n.d.	0	n.d.	n.d.
25	*m*-xylene			4±3	n.d.	n.d.	0	n.d.	n.d.	0	n.d.	n.d.
26	*p*-xylene	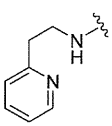	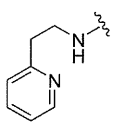	14±2	n.d.	n.d.	10±3	n.d.	n.d.	0	n.d.	n.d.
27	*m*-xylene			10±3	n.d.	n.d.	10±4	n.d.	n.d.	0	n.d.	n.d.
28	*p*-xylene	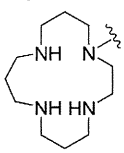	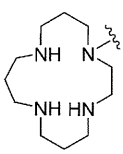	91±0.4	37±0.9	n.d.	97±4	>100	40	57±4	n.d.	n.d.
29	*m*-xylene			87±2	50±1	n.d.	>100	91±4	52	55±1	n.d.	n.d.
30	*p*-xylene	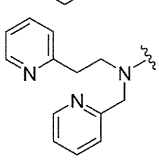	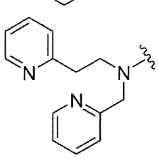	0	n.d.	n.d.	14±3	n.d.	n.d.	14±3	n.d.	n.d.
31	*m*-xylene			24±2	n.d.	n.d.	20±3	n.d.	n.d.	0	n.d.	n.d.
FC-131	*cyclo*-[D-Tyr-Arg-Arg-Nal-Gly-]			100	100	1.8	–	–	–	–	–	–

[a] CXCR4 binding activity was assessed based on inhibition of [^{125}I]CXCL12 binding to Jurkat cells. Percent inhibition for all compounds at 1 and 0.1 μM were calculated relative to the percent inhibition by FC131 (100%). [b] IC_{50} values are the concentrations which correspond to 50% inhibition of [^{125}I]CXCL12 binding to Jurkat cells. All data are mean values ±SEM of at least three independent experiments. n.d. = not determined.

affinities is commonly seen for these compounds and their zinc(II) or copper(II) complexes.

We investigated the CXCR4 antagonistic activity of compound **22** and the zinc complexes of **20**, **21**, **22**, and **28**, all of which possess strong CXCR4 binding activity. The CXCR4 antagonistic activity was assessed based on the inhibitory activity of the compounds against Ca^{2+} mobilization induced by CXCL12 stimulation through CXCR4 (figure S1 in the Support-

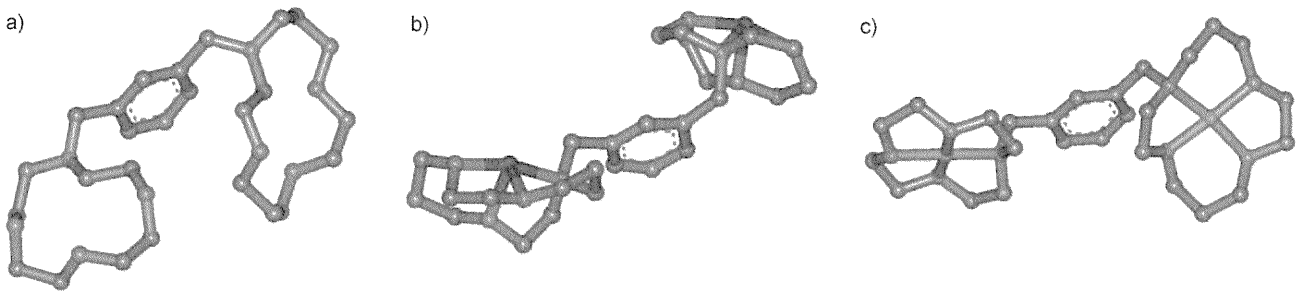

Figure 2. Structures calculated by molecular modeling of a) compound **21**, and its b) zinc and c) copper complexes. Atom color code: nitrogen = blue, carbon = gray, zinc = red, copper = light red.

ing Information). All of the tested compounds showed significant antagonistic activity at 1 μM.

The representative compounds **14**, **16**, **20–23**, **28**, and **29**, as well as their zinc chelates, were evaluated for anti-HIV activity. CXCR4 is the major co-receptor for the entry of T-cell-line-tropic (X4) HIV-1.[10,11] Inhibitory activity against X4-HIV-1 (NL4-3 strain)-induced cytopathogenicity in MT-4 cells was assessed and is shown in Table 2.[38] A correlation between CXCR4 binding activity and anti-HIV activity was observed. For compound **16** and its zinc complex, anti-HIV activity was significantly stronger than CXCR4 binding activity, and for the zinc complexes of compounds **20–22**, the CXCR4 binding activity is two to four-times stronger than the anti-HIV activity. The anti-HIV activity of the zinc complex of **16** was the most potent (EC_{50} = 8.2 nM). This is comparable to the anti-HIV activities of **16** and its zinc complex that were reported previously.[20,22,42,43] The zinc complex of **21**, which was the most active compound in terms of CXCR4 binding activity, also exhibited potent anti-HIV activity (EC_{50} = 36 nM).

Taken together, these results show that all of the compounds exhibiting CXCR4 binding activity also showed significant anti-HIV activity (EC_{50} values < 300 nM), and none of the tested compounds exhibited significant cytotoxicity (CC_{50} values > 10 μM; Table 2). Conversely, zinc complexes of **20**, **21**, **22**, and **28** did not exhibit significant anti-HIV activity against macrophage-tropic (R5) HIV-1 (NL(AD8) strain)-induced cytopathogenicity in PM-1 cells at concentrations below 10 μM. Since R5-HIV-1 strains use CCR5 instead of CXCR4 as the major co-receptor for entry, this suggests that these compounds do not bind CCR5 but rather are highly selective for CXCR4.

Table 2. Anti-HIV activity and cytotoxicity of representative compounds in the metal ion-free and zinc chelates.

Compd	Metal ion-free		Zinc chelate	
	EC_{50}[a] [nM]	CC_{50}[b] [μM]	EC_{50}[a] [nM]	CC_{50}[b] [μM]
14	200	> 10	200	> 10
16	21	> 10	8.2	> 10
20	38	> 10	39	> 10
21	50	> 10	36	> 10
22	93	> 10	48	> 10
23	290	> 10	220	> 10
28	36	> 10	56	> 10
29	130	> 10	42	> 10
FC131	93	> 10		
AZT	69	> 100		

[a] EC_{50} values are the concentrations corresponding to 50% protection from X4-HIV-1 (NL4–3 strain)-induced cytopathogenicity in MT-4 cells. [b] CC_{50} values are the concentrations at which the viability of MT-4 cells is reduced by 50%. All data are mean values from at least three independent experiments.

Conclusions

The present study introduces a new class of low-molecular-weight CXCR4 antagonists and their zinc(II) or copper(II) complexes, which contain pyridyl or azamacrocycle moieties with *p*-xylene or *m*-xylene spacers. These compounds demonstrated strong CXCR4 binding activity. Zinc complexes of **20** and **21**, which were the two most active compounds, contain cyclen and cyclam rings with *p*- and *m*-xylene spacers and exhibited remarkably potent IC_{50} values (11 and 8.3 nM, respectively). These compounds showed significant CXCR4 antagonistic activity, based on inhibitory activity against Ca^{2+} mobilization induced by CXCL12 stimulation through CXCR4, as well as potent anti-HIV activity, as assessed by protection from X4-HIV-1-induced cytopathogenicity in MT-4 cells. These results provide useful insights into the future design of novel CXCR4 antagonists, complementing information from other CXCR4 antagonists such as T140, FC131, and KRH-1636. Furthermore, these new compounds are useful for the development of therapeutic strategies for CXCR4-relevant diseases and chemical probes to study the biological activity of CXCR4.

Experimental Section

Chemistry

Compounds **12–17**, **20**, **21**, **24**, **25**, **27–29**, and **31** were synthesized as previously reported.[20,22,37,40,41,44–47] Compounds **18**, **19**, **22**, **23**, **26**, and **30** were synthesized in the present study; details are provided in the Supporting Information. A representative compound, **18**, was synthesized by coupling *p*-dibromoxylene (1,4-bis-(bromomethyl)benzene) with tri-Boc-protected 1,4,7,10-tetraazacyclododecane, followed by treatment with trifluoroacetic acid and subsequent coupling with bis(pyridin-2-ylmethyl)amine. All crude compounds were purified by RP-HPLC and identified by FAB/ESI-

HRMS. Zinc(II) or copper(II) complex formation was accomplished by treatment of the above compounds with 10 equiv of $ZnCl_2$ or $CuCl_2$ in PBS. All zinc(II) or copper(II) complexes were characterized by chemical shifts of their methylene protons in ^1H NMR analysis. The pyridyl zinc(II) complex was characterized previously,[37] and zinc(II) or copper(II) complex formation with these macrocyclic compounds has been reported elsewhere.[41,42,48,49] Detailed procedures and data are provided in the Supporting Information.

Biological assays

A CXCR4 binding assay for compounds, based on the inhibition of [^{125}I]CXCL12 binding to Jurkat cells, was performed as reported by Tanaka et al.[38] CXCR4 antagonistic activity was evaluated as described by Ichiyama et al[27], measuring inhibitory activity against Ca^{2+} mobilization induced by CXCL12 stimulation in HOS cells expressing CXCR4. Anti-HIV activity was determined by inhibitory activity against X4-HIV-1(NL4–3)-induced cytopathogenicity in MT-4 cells as reported by Tanaka et al.[38] An X4 HIV-1 infectious molecular clone (pNL4–3) was obtained from the AIDS Research and Reference Reagent Program. The virus NL4–3 was obtained from the culture supernatant of 293T cells transfected with pNL4–3.

Molecular modeling

Molecular modeling calculations were performed using Sybyl (version 7.0, Tripos). Energy minimization was performed using the Tripos force field and Gasteiger–Hückel charge parameters. The lowest energy conformation was obtained by random search methods.

Acknowledgements

T.T. and N.O. are supported by research fellowships for young scientists from the Japan Society for the Promotion of Science. This work was supported in part by a Grant-in-Aid for Scientific Research from the Ministry of Education, Culture, Sports, Science, and Technology of Japan, and Health and Labor Sciences Research Grants from the Japanese Ministry of Health, Labor, and Welfare. The authors thank Mr. Wu Honggui (Tokyo University of Science) for his assistance with the anti-HIV assay.

Keywords: azamacrocycles · Ca^{2+} mobilization · CXCR4 · HIV · structure–activity relationships

[1] T. Nagasawa, H. Kikutani, T. Kishimoto, *Proc. Natl. Acad. Sci. USA* **1994**, *91*, 2305–2309.
[2] C. C. Bleul, M. Farzan, H. Choe, C. Parolin, I. Clark-Lewis, J. Sodroski, T. A. Springer, *Nature* **1996**, *382*, 829–833.
[3] E. Oberlin, A. Amara, F. Bachelerie, C. Bessia, J. L. Virelizier, F. Arenzana-Seisdedos, O. Schwartz, J. M. Heard, I. Clark-Lewis, D. L. Legler, M. Loetscher, M. Baggiolini, B. Moser, *Nature* **1996**, *382*, 833–835.
[4] K. Tashiro, H. Tada, R. Heilker, M. Shirozu, T. Nakano, T. Honjo, *Science* **1993**, *261*, 600–603.
[5] C. C. Bleul, R. C. Fuhlbrigge, J. M. Casanovas, A. Aiuti, T. A. Springer, *J. Exp. Med.* **1996**, *184*, 1101–1109.
[6] K. Tachibana, S. Hirota, H. Iizasa, H. Yoshida, K. Kawabata, Y. Kataoka, Y. Kitamura, K. Matsushima, N. Yoshida, S. Nishikawa, T. Kishimoto, T. Nagasawa, *Nature* **1998**, *393*, 591–594.
[7] T. Nagasawa, S. Hirota, K. Tachibana, N. Takakura, S. Nishikawa, Y. Kitamura, N. Yoshida, H. Kikutani, T. Kishimoto, *Nature* **1996**, *382*, 635–638.
[8] Y. Zhu, Y. Yu, X. C. Zhang, T. Nagasawa, J. Y. Wu, Y. Rao, *Nat. Neurosci.* **2002**, *5*, 719–720.
[9] R. K. Stumm, C. Zhou, T. Ara, F. Lazarini, M. Dubois-Dalcq, T. Nagasawa, V. Hollt, S. Schulz, *J. Neurosci.* **2003**, *23*, 5123–5130.
[10] H. K. Deng, R. Liu, W. Ellmeier, S. Choe, D. Unutmaz, M. Burkhart, P. D. Marzio, S. Marmon, R. E. Sutton, C. M. Hill, C. B. Davis, S. C. Peiper, T. J. Schall, D. R. Littman, N. R. Landau, *Nature* **1996**, *381*, 661–666.
[11] Y. Feng, C. C. Broder, P. E. Kennedy, E. A. Berger, *Science* **1996**, *272*, 872–877.
[12] T. Koshiba, R. Hosotani, Y. Miyamoto, J. Ida, S. Tsuji, S. Nakajima, M. Kawaguchi, H. Kobayashi, R. Doi, T. Hori, N. Fujii, M. Imamura, *Clin. Cancer Res.* **2000**, *6*, 3530–3535.
[13] A. Müller, B. Homey, H. Soto, N. Ge, D. Catron, M. E. Buchanan, T. McClanahan, E. Murphy, W. Yuan, S. N. Wagner, J. L. Barrera, A. Mohar, E. Verastegui, A. Zlotnik, *Nature* **2001**, *410*, 50–56.
[14] H. Tamamura, A. Hori, N. Kanzaki, K. Hiramatsu, M. Mizumoto, H. Nakashima, N. Yamamoto, A. Otaka, N. Fujii, *FEBS Lett.* **2003**, *550*, 79–83.
[15] N. Tsukada, J. A. Burger, N. J. Zvaifler, T. J. Kipps, *Blood* **2002**, *99*, 1030–1037.
[16] J. Juarez, K. F. Bradstock, D. J. Gottlieb, L. J. Bendall, *Leukemia* **2003**, *17*, 1294–1300.
[17] T. Nanki, K. Hayashida, H. S. El-Gabalawy, S. Suson, K. Shi, H. J. Girschick, S. Yavuz, P. E. Lipsky, *J. Immunol.* **2000**, *165*, 6590–6598.
[18] H. Tamamura, M. Fujisawa, K. Hiramatsu, M. Mizumoto, H. Nakashima, N. Yamamoto, A. Otaka, N. Fujii, *FEBS Lett.* **2004**, *569*, 99–104.
[19] T. Murakami, T. Nakajima, Y. Koyanagi, K. Tachibana, N. Fujii, H. Tamamura, N. Toshida, M. Waki, A. Matsumoto, O. Yoshie, T. Kishimoto, N. Yamamoto, T. Nagasawa, *J. Exp. Med.* **1997**, *186*, 1389–1393.
[20] D. Schols, S. Struyf, J. Van Damme, J. A. Este, G. Henson, E. DeClarcq, *J. Exp. Med.* **1997**, *186*, 1383–1388.
[21] B. J. Doranz, K. Grovit-Ferbas, M. P. Sharron, S.-H. Mao, M. Bidwell Goetz, E. S. Daar, R. W. Doms, W. A. O'Brien, *J. Exp. Med.* **1997**, *186*, 1395–1400.
[22] G. A. Donzella, D. Schols, S. W. Lin, J. A. Este, K. A. Nagashima, *Nat. Med.* **1998**, *4*, 72–76.
[23] O. M. Z. Howard, J. J. Oppenheim, M. G. Hollingshead, J. M. Covey, J. Bigelow, J. J. McCormack, R. W. Buckheit, Jr., D. J. Clanton, J. A. Turpin, W. G. Rice, *J. Med. Chem.* **1998**, *41*, 2184–2193.
[24] H. Tamamura, Y. Xu, T. Hattori, X. Zhang, R. Arakaki, K. Kanbara, A. Omagari, A. Otaka, T. Ibuka, N. Yamamoto, H. Nakashima, N. Fujii, *Biochem. Biophys. Res. Commun.* **1998**, *253*, 877–882.
[25] H. Tamamura, A. Omagari, S. Oishi, T. Kanamoto, N. Yamamoto, S. C. Peiper, H. Nakashima, A. Otaka, N. Fujii, *Bioorg. Med. Chem. Lett.* **2000**, *10*, 2633–2637.
[26] N. Fujii, S. Oishi, K. Hiramatsu, T. Araki, S. Ueda, H. Tamamura, A. Otaka, S. Kusano, S. Terakubo, H. Nakashima, J. A. Broach, J. O. Trent, Z. Wang, S. C. Peiper, *Angew. Chem.* **2003**, *115*, 3373–3375; *Angew. Chem. Int. Ed.* **2003**, *42*, 3251–3253.
[27] K. Ichiyama, S. Yokoyama-Kumakura, Y. Tanaka, R. Tanaka, K. Hirose, K. Bannai, T. Edamatsu, M. Yanaka, Y. Niitani, N. Miyano-Kurosaki, H. Takaku, Y. Koyanagi, N. Yamamoto, *Proc. Natl. Acad. Sci. USA* **2003**, *100*, 4185–4190.
[28] H. Tamamura, N. Fujii, *Curr. Drug Targets-Infectious Disorders* **2004**, *4*, 103–110.
[29] H. Tamamura, K. Hiramatsu, S. Ueda, Z. Wang, S. Kusano, S. Terakubo, J. O. Trent, S. C. Peiper, N. Yamamoto, H. Nakashima, A. Otaka, N. Fujii, *J. Med. Chem.* **2005**, *48*, 380–391.
[30] H. Tamamura, T. Araki, S. Ueda, Z. Wang, S. Oishi, A. Esaka, J. O. Trent, H. Nakashima, N. Yamamoto, S. C. Peiper, A. Otaka, N. Fujii, *J. Med. Chem.* **2005**, *48*, 3280–3289.
[31] G. C. Valks, G. McRobbie, E. A. Lewis, T. J. Hubin, T. M. Hunter, P. J. Sadler, C. Pannecouque, E. De Clercq, S. J. Archibald, *J. Med. Chem.* **2006**, *49*, 6162–6165.
[32] W. Zhan, Z. Liang, A. Zhu, S. Kurtkaya, H. Shim, J. P. Snyder, D. C. Liotta, *J. Med. Chem.* **2007**, *50*, 5655–5664.
[33] A. Khan, G. Nicholson, J. Greenman, L. Madden, G. McRobbie, C. Pannecouque, E. De Clercq, R. Ullom, D. L. Maples, R. D. Maples, J. D. Silversides, T. J. Hubin, S. J. Archibald, *J. Am. Chem. Soc.* **2009**, *131*, 3416–3417.
[34] G. J. Bridger, R. T. Skerlj, P. E. Hernandez-Abad, D. E. Bogucki, Z. Wang, Y. Zhou, S. Nan, E. M. Boehringer, T. Wilson, J. Crawford, M. Metz, S. Hatse, K. Princen, E. De Clercq, D. Schols, *J. Med. Chem.* **2010**, *53*, 1250–1260.

[35] R. T. Skerlj, G. J. Bridger, A. Kaller, E. J. McEachern, J. B. Crawford, Y. Zhou, B. Atsma, J. Langille, S. Nan, D. Veale, T. Wilson, C. Harwig, S. Hatse, K. Princen, E. De Clercq, D. Schols, *J. Med. Chem.* **2010**, *53*, 3376–3388.
[36] M. Takenaga, H. Tamamura, K. Hiramatsu, N. Nakamura, Y. Yamaguchi, A. Kitagawa, S. Kawai, H. Nakashima, N. Fujii, R. Igarashi, *Biochem. Biophys. Res. Commun.* **2004**, *320*, 226–232.
[37] H. Tamamura, A. Ojida, T. Ogawa, H. Tsutsumi, H. Masuno, H. Nakashima, N. Yamamoto, I. Hamachi, N. Fujii, *J. Med. Chem.* **2006**, *49*, 3412–3415.
[38] T. Tanaka, H. Tsutsumi, W. Nomura, Y. Tanabe, N. Ohashi, A. Esaka, C. Ochiai, J. Sato, K. Itotani, T. Murakami, K. Ohba, N. Yamamoto, N. Fujii, H. Tamamura, *Org. Biomol. Chem.* **2008**, *6*, 4374–4377.
[39] G. J. Bridger, R. T. Skerlj, D. Thornton, S. Padmanabhan, S. A. Martellucci, G. W. Henson, M. J. Abrams, N. Yamamoto, K. De Vreese, R. Pauwels, E. De Clercq, *J. Med. Chem.* **1995**, *38*, 366–378.
[40] G. J. Bridger, R. T. Skerlj, S. Padmanabhan, S. A. Martellucci, G. W. Henson, M. J. Abrams, H. C. Joao, M. Witvrouw, K. De Vreese, R. Pauwels, E. De Clercq, *J. Med. Chem.* **1996**, *39*, 109–119.
[41] Y. Inouye, T. Kanamori, T. Yoshida, T. Koike, M. Shionoya, H. Fujioka, E. Kimura, *Biol. Pharm. Bull.* **1996**, *19*, 456–458.
[42] L. O. Gerlach, J. S. Jakobsen, K. P. Jensen, M. R. Rosenkilde, R. T. Skerlj, U. Ryde, G. J. Bridger, T. W. Schwartz, *Biochemistry* **2003**, *42*, 710–717.
[43] H. F. Egberink, E. De Clercq, A. L. Van Vliet, J. Balzarini, G. J. Bridger, G. Henson, M. C. Horzinek, D. Schols, *J. Virol.* **1999**, *73*, 6346–6352.
[44] M. Le Baccon, F. Chuburu, L. Toupet, H. Handel, M. Soibinet, I. Dechamps-Olivier, J.-P. Barbier, M. Aplincourt, *New J. Chem.* **2001**, *25*, 1168–1174.
[45] B. Antonioli, D. J. Bray, J. K. Clegg, K. Gloe, K. Gloe, O. Kataeva, L. F. Lindoy, J. C. McMurtrie, P. J. Steel, C. J. Sumby, M. Wenzel, *Dalton Trans.* **2006**, 4783–4794.
[46] S. P. Foxon, D. Utz, J. Astner, S. Schindler, F. Thaler, F. W. Heinemann, G. Liehr, J. Mukherjee, V. Balamurugan, D. Ghosh, R. Mukherjee, *Dalton Trans.* **2004**, 2321–2328.
[47] S. Mandal, F. Lloret, R. Mukherjee, *Inorg. Chim. Acta* **2009**, *362*, 27–37.
[48] M. Soibinet, I. De'champs-Olivier, E. Guillon, J.-P. Barbier, M. Aplincourt, F. Chuburu, M. Le Baccon, H. Handel, *Eur. J. Inorg. Chem.* **2003**, 1984–1994.
[49] R. W. Hay, M. T. Tarafder, *Transition Met. Chem.* **1990**, *15*, 490–492.

Received: December 19, 2010
Published online on February 10, 2011

Bioconjugate Chemistry

ARTICLE

pubs.acs.org/bc

Fluorescence-Quenching Screening of Protein Kinase C Ligands with an Environmentally Sensitive Fluorophore

Wataru Nomura,[†] Nami Ohashi,[†] Yoshiaki Okuda,[†,‡] Tetsuo Narumi,[†] Teikichi Ikura,[‡] Nobutoshi Ito,[‡] and Hirokazu Tamamura*[,†,‡]

[†]Department of Medicinal Chemistry, Institute of Biomaterials and Bioengineering, Tokyo Medical and Dental University, 2-3-10 Kandasurugadai, Chiyoda-ku, Tokyo 101-0062, Japan

[‡]Graduate School of Biomedical Science, Tokyo Medical and Dental University, 1-5-45 Yushima, Bunkyo-ku, Tokyo 113-8510, Japan

Supporting Information

ABSTRACT: A novel fluorescence-quenching screening method for protein kinase C (PKC) ligands was developed utilizing solvatochromic fluorophores. Solvatochromic dyes, highly sensitive to the presence or the absence of competitive ligands in their binding to the C1b domain of PKCδ (δC1b), were combined with a known pharmacophoric moiety of 1,2-diacylglycerol (DAG) lactones, PKC ligands. Addition of δC1b to the fluorescent compounds caused a gradual increase in the fluorescent intensity in proportion to the increase of δC1b. As a competitive ligand was added to the complex of δC1b domain and fluorescent compounds, a gradual decrease in the fluorescent intensity was observed. The relative binding affinities of known ligands were successfully determined by this fluorescent method and corresponded well to the K_i values measured by a radioisotope method. These results indicate that washing, which is a laborious step in binding evaluations, is not required for this environmentally sensitive fluorophore based system. Screening with the system was performed for 2560 preselected library compounds with possible pharmacophores, and some lead compounds were found. This fluorescence-based method could be applied widely to known ligand−receptor combinations.

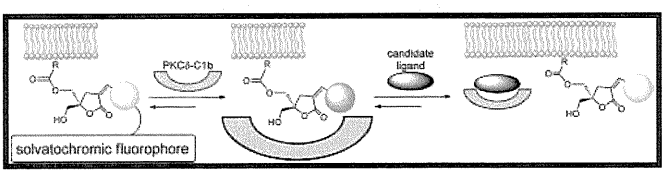

INTRODUCTION

Solvatochromic fluorophores are sensitive to immediate changes in their environment such as binding of ligands to proteins,[1] and significant biological issues have been examined by chemical probes with fluorescent dyes.[2,3] The major advantage of the fluorescence-based methods in the observation of physiological phenomena in cells is that detection and evaluation can be performed in real-time directly by microscopy. In these techniques, the signal/background ratio is critical to avoid the observation of artifacts or to obtain clearer images at high resolution. Screening methods of bioactive compounds have been developed as another application of fluorescence.[4] From the aspect of sensitivity, radioisotope (RI) based methods are more efficient but involve laborious experimental procedures. For the development of convenient screening procedures, a simple method for evaluation of binding is needed. By attachment of solvatochromic fluorophores to known ligands, the binding affinity of unknown ligands can be evaluated and related to RI methods.[5] Fluorescent intensity is highly dependent on the binding state to a target protein, and the signal/background ratio would be sufficient without washing steps, which are normally necessary in fluorescent analysis.[6,7]

In this study, we have developed reporter compounds containing solvatochromic dyes for the detection of ligand binding to a target protein and applied them to the screening of chemical libraries. Protein kinase Cδ (PKCδ) was chosen as a target protein because of its importance in physiological phenomena. The 11 isozymes that constitute PKC play pivotal roles in physiological responses to growth factors, oxidative stress, 1,2-diacylglycerol (DAG), and tumor promoters, such as phorbol esters. These responses regulate numerous cellular processes,[8,9] including proliferation,[10] differentiation,[11] migration,[12] and apoptosis.[13,14] Membrane translocation of PKC is caused by binding of ligands to the C1b domain and has been recognized as an important phenomenon in signal transduction because the localization of PKC is key in determining isozyme-specific functions by defining binding partners for downstream signaling.[15] Despite the complex regulatory mechanisms of PKC activation, considerable progress has been made in understanding isozyme-specific functions[16] and several ligands with high specificity for PKC isozymes have been developed as potential drugs.[17−23] Through the development of DAG-lactones, whose design is based on the endogenous ligand DAG, the importance of maintaining intact the pharmacophore triad of two carbonyl groups (*sn*-1 and *sn*-2) and the primary alcohol has been established as a requirement in high affinity ligands for PKC (Figure 1).[16] Various PKC ligands have been synthesized and found to be inhibitors of tumor promotion or of other diseases.

Received: December 13, 2010
Revised: March 13, 2011
Published: March 25, 2011

However, there are limitations to the design of compound templates so far. Thus, in this study, we have attempted to develop the screening methods aimed at discovery of novel template structures for PKCδ ligands as drug leads.

EXPERIMENTAL PROCEDURES

General. ^{1}H NMR spectra were recorded using a Bruker AV500 spectrometer. Chemical shifts were reported in δ (ppm) relative to Me_4Si (in $CDCl_3$) as an internal standard. Low- and high-resolution mass spectra were recorded on a JMS-T1000LC AccuTOF and Bruker Daltonics microTOF-2focus in both positive and negative detection modes. Wakogel C-200 (Wako Pure Chemical Industries, Ltd.) and silica gel 60 N (Kanto Chemical Co., Inc.) were employed for flash chromatography. Fluorescent spectra were recorded on a JASCO FP-6600 spectrofluorometer and JASCO V-650 spectrophotometer using a quartz cell with 1.0 cm path length. Fluorescent intensities of samples in 96-well plates were recorded on Wallac ARVO MX.

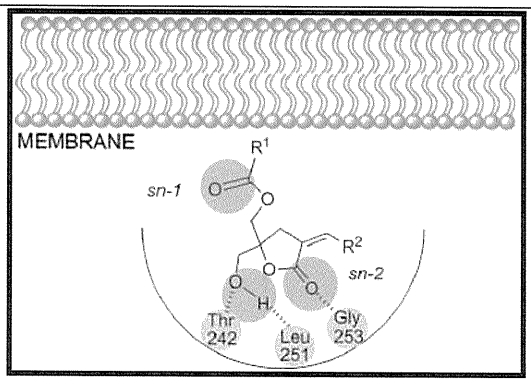

Figure 1. Binding mode of DAG-lactone derivatives to the δC1b domain. The *sn*-1 and *sn*-2 carbonyl groups are indicated. Three important pharmacophores are indicated by light blue spheres. Amino acid residues interacting with these pharmacophores (threonine at 242, leucine at 251, and glycine at 253) are indicated by red spheres.

Standard Monoacylation Procedure. Under argon, Et_3N (3 equiv) was added at 0 °C to a solution containing 5,5-bis(hydroxymethyl)oxalan-2-one in THF, and the mixture was stirred at 0 °C for 30 min. Then 0.2−1.1 equiv of a carboxylic acid derivative (an acyl chloride or carboxylic anhydride) was added. This mixture was stirred at 0 °C for a further 4 h. After evaporation of the solvent, the obtained residue was purified by flash column chromatography.

Preparation of Compounds 7, 10−13, 16, 17, and 19−21. Compounds **7**, **10**−**12**, and **16** were prepared as described in ref 17. Compounds **13** and **17** were prepared as described in refs 24 and 25. The synthesis of **19** is described elsewhere.[26] Compounds **20** and **21** are commercially available.

Expression and Purification of the δC1b Domain. DNA coding C1b domain of mouse PKCδ (231−280)[27] was subcloned into *Bam*H1 and *Eco*RI sites of pGEX-2tk (GE Healthcare) and expressed as gluthatione-*S*-transferase (GST) fusion protein in *Escherichia coli* C41 which contains extension sequences Gly-Ser-Arg-Arg-Ala-Ser-Val-Gly-Ser and Glu-Phe-Ile-Val-Thr-Asp at the N- and C-termini, respectively. The δC1b

Scheme 1. Synthesis of Fluorescent Compounds 1−3[a]

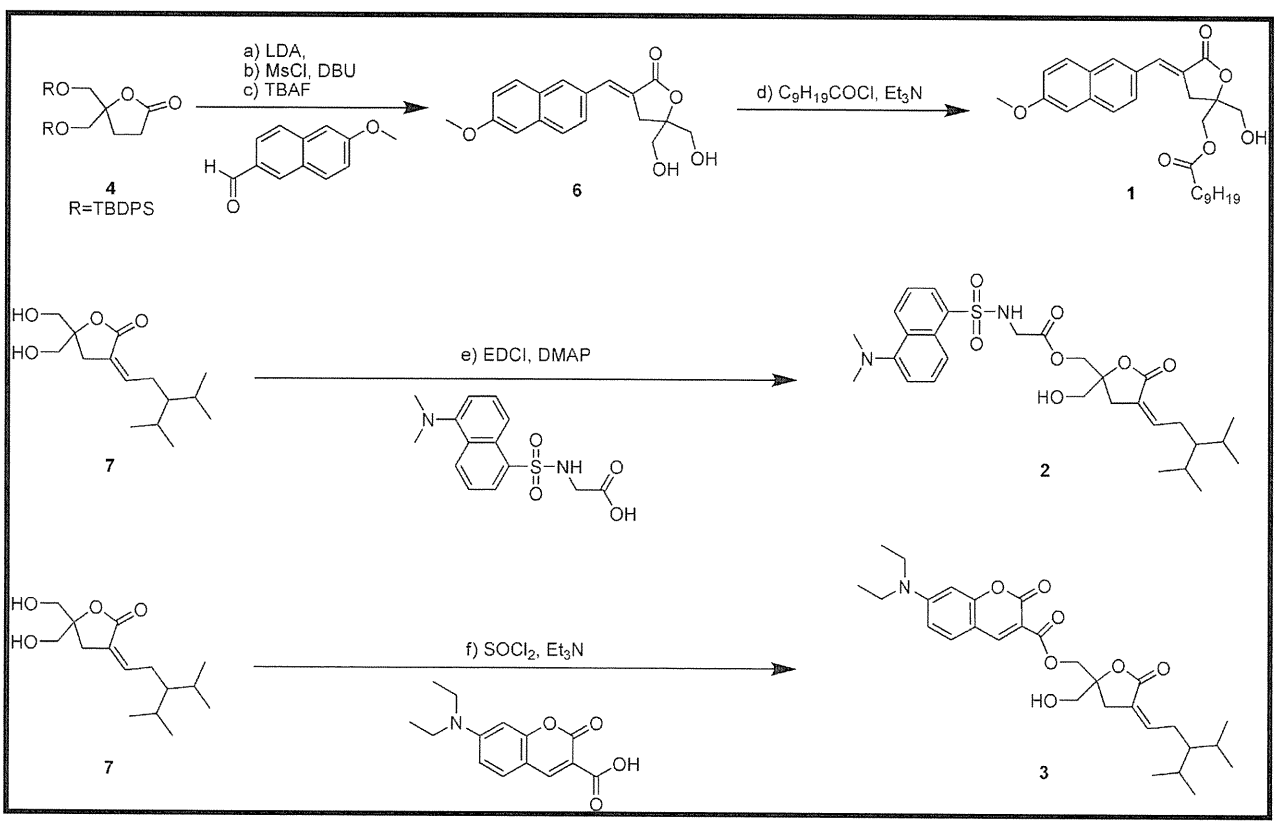

[a] (a) LDA, −78 °C; (b) MsCl, DBU, 0 °C to room temp; (c) TBAF, 0 °C to room temp; (d) $C_9H_{19}COCl$, Et_3N, 0 °C; (e) EDCI, DMAP, 0 °C; (f) $SOCl_2$, Et_3N, 0 °C.

dx.doi.org/10.1021/bc100567k |*Bioconjugate Chem.* 2011, 22, 923–930

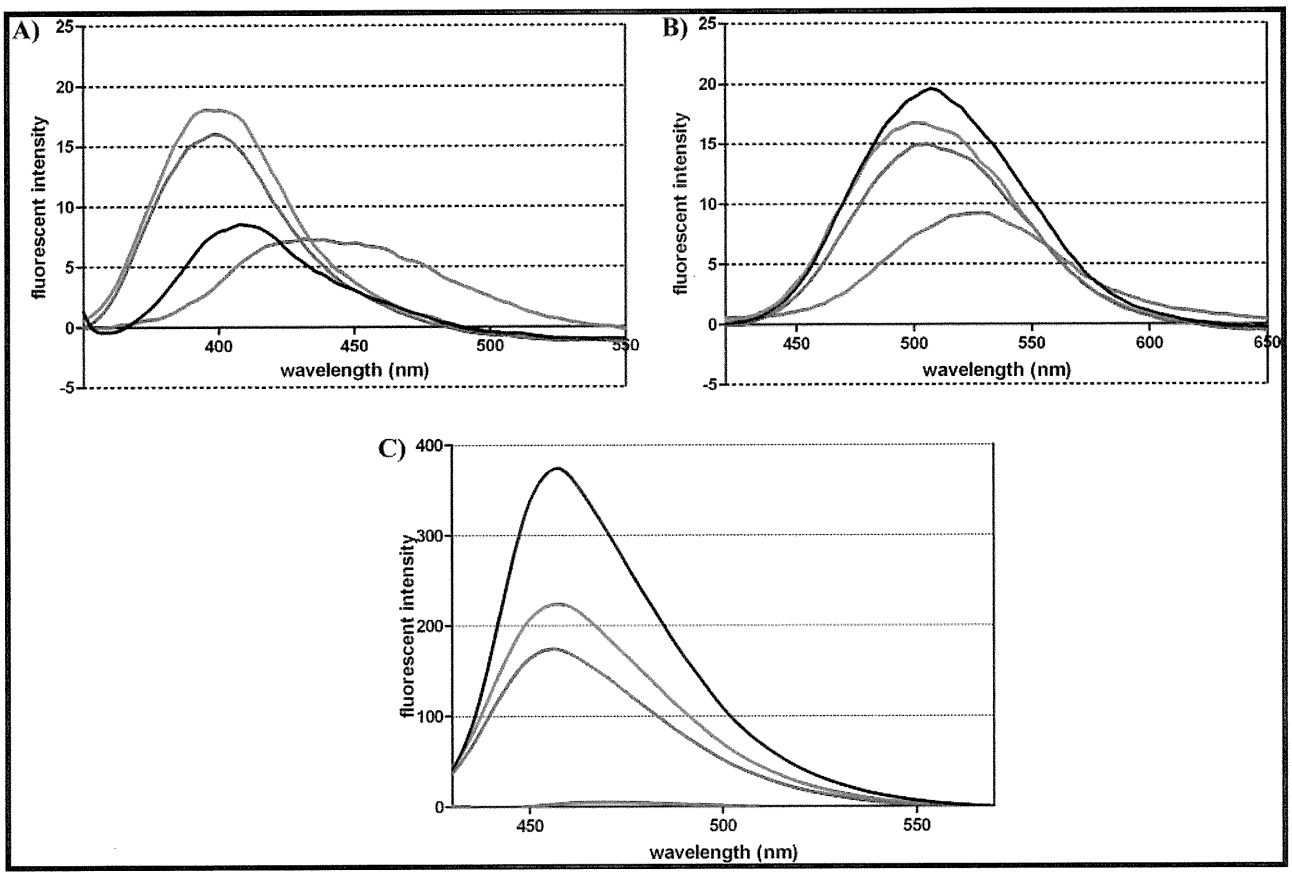

Figure 2. Fluorescent spectra of compounds **1** (A), **2** (B), and **3** (C) in different solvents. The spectra show fluorescence in the solvents color-coded as follows: red, MeOH; blue, THF; black, $CHCl_3$; green, EtOAc. Each ligand was prepared as 1 mM solution in DMSO. In UV measurement, 10 μL of ligand was added to 990 μL of solvents.

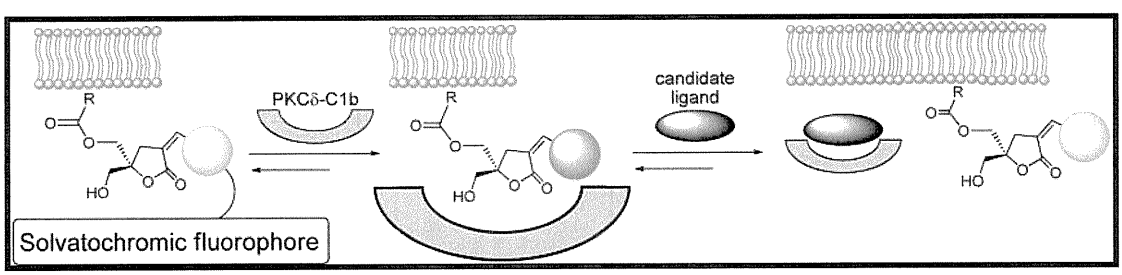

Figure 3. Schematic representation of a fluorescence-quenching screening system. In the presence of the δC1b domain, fluorescence of a solvatochromic fluorophore is enhanced. The replacement by candidate compounds results in fluorescence quenching.

Table 1. Changes of Fluorescent Intensity upon δC1b Binding and Inhibition Constants to δC1b Determined by Competition Assay against [^{3}H]PDBu

compd	ΔF [a]	K_i (nM) [b]
1	3.8	35.9
2	2.3	368
3	0.50	93.3

[a] Fluorescent change by binding of the δC1b domain. The values were determined by titration of the δC1b domain. The ΔF was determined by dividing F_1 by F_0 at the maximum of fluorescent emission in each spectrum. [b] Inhibitory constants determined by competition analysis against [^{3}H]PDBu.[28,36,37]

domain after cleavage contains 65 amino acid residues. Cells were grown at 37 °C in LB medium and induced with 0.3 mM IPTG at growth phase. Cells were cultured overnight at 20 °C after induction. Cells were collected and lysed in 50 mM Tris·HCl buffer (pH 8.0) containing 100 mM NaCl, 1 μg/mL leupeptine, 1 mM PMSF, and 1 mM DTT. Expressed protein was extracted by sonication, then purified by affinity chromatography utilizing glutathione-Sepharose 4B beads resin. GST moiety was cleaved by 300 units of thrombin at 4 °C overnight. The cleaved protein was eluted and further purified on a 2.6 cm × 60 cm Superdex S-75 gel filtration column. Purification was by FPLC system at a flow rate of 1 mL/min utilizing 0.1 M triethanolamine·HCl (pH 7.0) containing 0.5 M NaCl.

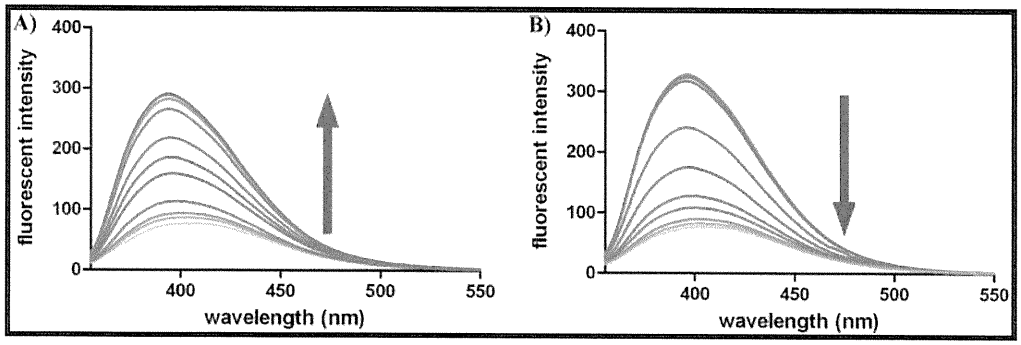

Figure 4. Changes of fluorescent spectra of compound **1** during titration of the δC1b domain (A) and during titration of PDBu (compound **8**) (B) after δC1b binding. The concentration of the δC1b domain was increased to 1.28 μM (6.4 equiv to compound **1**) by titration. The concentration of PDBu was increased to 10.2 μM (51.2 equiv to compound **1**) by titration.

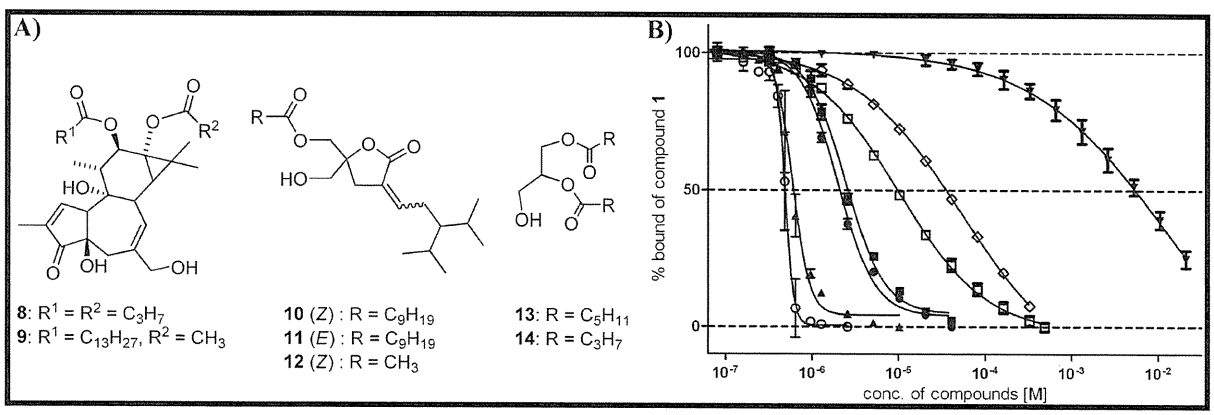

Figure 5. Competitive assay against compound **1** based on fluorescent intensity (spectrofluorometer). (A) Structures of test compounds. (B) Inhibition curves indicate results of compounds **8** (▲), **9** (○), **10** (●), **11** (■), **12** (□), **13** (◇), and **14** (▼).

Determination of K_i of Compounds for Full Length PKCδ. Enzyme–ligand interaction was assessed in vitro as the ability of the ligand to displace bound [20-^{3}H]phorbol 12,13-dibutyrate ([^{3}H]PDBu) from recombinant human PKCδ in the presence of phosphatidylserine (PS) in an experimental procedure that was described previously.[28] In constant concentration analysis, the concentrations of compounds were fixed at 100 nM for known compounds and at 10 μM for library compounds. The other procedures were the same as those of the standard evaluation.

Fluorescent Titration of the δC1b Domain. An amount of 25 μL of a solution of PS in chloroform (10 mg/mL) was evaporated to dryness under nitrogen. Then 50 mM Tris·HCl buffer (pH 7.4) was added and the PS was sonicated with a Microtip for a total of 15 s. A stock solution of compound **1** was diluted with 50 mM Tris·HCl buffer (pH 7.4) containing 100 μg/mL PS to prepare a 0.2 μM solution. The recombinant δC1b domain was added to the 0.2 μM solution of compound **1**, and fluorescent spectra (λ_{ex} = 340 nm) were measured at 25 °C. The concentration of the recombinant δC1b domain started at 0.01 μM and increased to 1.28 μM by titration. The final concentrations of compounds **2** and **3** were 0.2 and 0.05 μM, respectively. Change of fluorescent intensity (ΔF) was calculated at the following wavelengths, which showed λ_{max} in each evaluation; compound **1**, 406 (F_0) and 394 (F_1) nm; compound **2**, 520 (F_0) and 480 (F_1) nm; compound **3**, 463 (F_0) and 461 (F_1) nm. Wavelengths recorded before and after the addition of the δC1b domain.

Fluorescent Titration of Candidate Ligands. Compound **1** was diluted with 50 mM Tris·HCl (pH 7.4) containing 100 μg/mL PS to obtain a solution with a 0.2 μM final concentration. The δC1b domain was added to the above solution of compound **1** to be 0.96 μM. A candidate ligand was added to the solution, and fluorescent spectra were recorded with a spectrofluorometer at 25 °C. Fluorescent titration curves (λ_{em} = 407 nm) were analyzed by nonlinear regression, and IC_{50} values were estimated by a nonlinear least-squares curve-fitting method using GraphPad Prism 5 (GraphPad Software, Inc., La Jolla, CA, U.S.). In the constant concentration analysis, the concentrations of known compounds were fixed at 100 nM and of library compounds at 10 μM. The other procedures were the same as those in the standard evaluation.

Fluorescence-Quenching Analysis for Library Screening Recorded by Microplate Reader. Fluorescence intensity was recorded on Wallac ARVO MX (PerkinElmer) using a 96-well black plate. Compound **1** was diluted with 50 mM Tris·HCl (pH 7.4) containing 100 μg/mL PS to obtain a solution with a 0.2 μM final concentration. The δC1b domain was added to the above solution of compound **1** to be 0.96 μM. A candidate ligand (10 μM) was added to the compound **1**–δC1b domain complex solution, and fluorescent intensities (λ_{ex} = 355 nm, λ_{em} = 405 nm) were measured at 25 °C.

RESULTS AND DISCUSSION

Synthesis and Fluorescent Properties of Compounds 1–3. Three representative solvatochromic fluorophores, involving 6-methoxynaphthalene,[29] 5-(dimethylamino)naphthalene-1-sulfonyl (dansyl),[6,30,31] and diethylaminocoumarin,[32–35] have

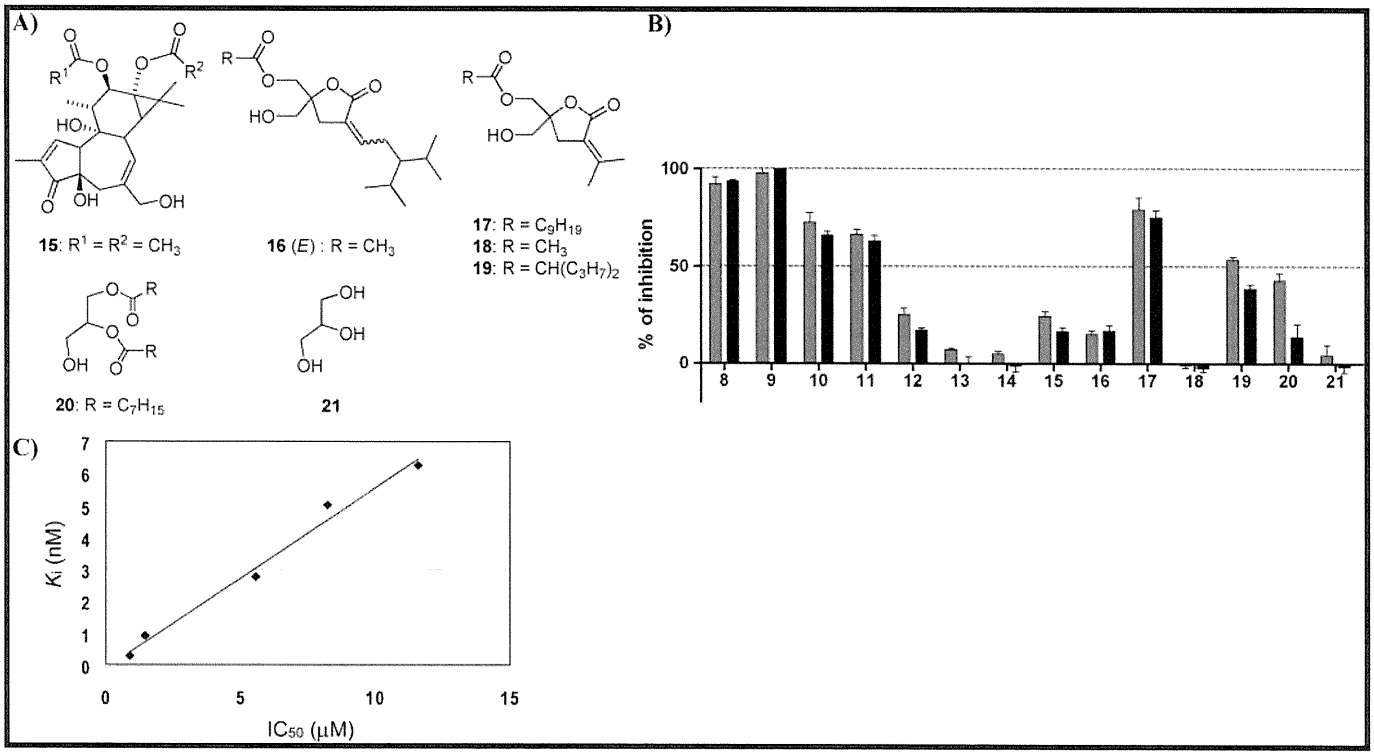

Figure 6. Comparison of inhibition percentages between the fluorescent assay (microplate reader) and the RI assay at a constant concentration of test compounds. (A) Structures of test compounds. (B) Inhibition of binding of compound **1** (fluorescent assay, left gray bars) or [^{3}H]PDBu (RI assay, right black bars) in the presence of test compounds (10 μM in the fluorescent assay and 100 nM in the RI assay). The final DMSO concentration is 4%. (C) Plots of IC_{50} values (μM) by the fluorescent assay versus K_i (nM) by the RI assay for compounds **8**, **9**, **10**, **11**, and **17**.

been utilized. The 6-methoxynaphthalene was incorporated at the α-carbon of the *sn*-1 carbonyl group of the DAG-lactone structure (Scheme 1). The dansyl and diethylaminocoumarin were incorporated into the *sn*-2 carbonyl group. In comparison with the fluorescent spectra of these compounds, obtained in various solvents, compound **1** showed the most variation with solvent polarity (Figure 2). It is known that solvatochromic fluorophores show higher fluorescent intensity in hydrophobic environments and that the fluorophores are sensitive to the environment of a binding pocket in target proteins. The fluorescent intensity of labeled DAG-lactones should reflect its binding to a target protein, PKCδ (Figure 3), and as expected, our reporter compounds **1** and **2** containing solvatochromic fluorophores exibited a remarkable increase of fluorescent intensity in the proximity of the C1b domain of PKCδ (δC1b), which is a specific target of DAG-lactone derivatives (Table 1 and Figure 4A). This indicates that in the binding of compounds **1** and **2** to the δC1b domain, the 6-methoxynaphthalene and dansyl moieties are located in the hydrophobic environment. However, for compound **3**, the fluorescent intensity was decreased as the concentration of δC1b increased. The spectra in various solvents showed dependence of the fluorescent intensity of the compound **3** on solvent polarity, and it was suggested that in the binding of compound **3** to the δC1b domain, the diethylaminocoumarin moiety could be located in the hydrophilic environment. The changes of fluorescent intensity of the synthetic compounds are summarized in Table 1. The binding constants of fluorescent compounds were evaluated by [^{3}H]PDBu competitive assay. Compound **1** showed the highest binding affinity for the δC1b domain. In the fluorescence-based analysis of binding, two factors are key to the sensitivity of the assay system: (i) the fluorescent change as a function of the ligand binding and (ii) the binding affinity of a reporter compound.

Evaluation of Binding to PKCδ by Fluorescent Change of Compound 1. The results obtained supported the selection of compound **1** as a reporter compound for further study. In competitive assays, when candidate ligands of PKCδ are present, they replace the fluorescent compounds, which are formerly bound to δC1b, and the fluorescent intensity should decrease. Practically, addition of PDBu to the complex of compound **1** and δC1b resulted in a remarkable decrease of fluorescent intensity (Figure 4B). By utilization of compound **1** as a reporter, binding analysis of known PKCδ ligands was performed to assess the reliability of the assay system. Compounds **8**−**14** were prepared as test compounds (Figure 5A), and their IC_{50} values, determined by the fluorescence-based competitive assay with a fluorospectrophotometer against compound **1**, were 0.60, 0.49, 1.95, 2.42, 10.0, 54.2, and 1.22 × 10^4 μM, respectively (Figure 5B). The order of the IC_{50} values of compounds **8**−**11** is identical to that of the K_i values (0.91, 0.26, 5.0, and 6.2 nM, respectively) determined by the [^{3}H]PDBu competitive assay.

The Binding Analysis by Competition with Compound 1 Showed Linearity with the Classical RI Assay. To further assess the collinearity of the fluorescent assay on microplates and the [^{3}H]PDBu assay, the inhibition percentages by compounds **8**−**21** in both assays (Figure 6A) at constant concentration were compared. The compound concentrations were set at 10 μM for the fluorescent assay and at 100 nM for the [^{3}H]PDBu assay. As shown in Figure 6B, the inhibition percentages of compounds **8**−**21** are similar in both assays. Comparison of the IC_{50} and K_i of compounds **8**, **9**, **10**, **11**, and **17**, possessing more than 60% inhibition percentages, showed acceptable linearity (Figure 6C).

dx.doi.org/10.1021/bc100567k |*Bioconjugate Chem.* 2011, 22, 923–930

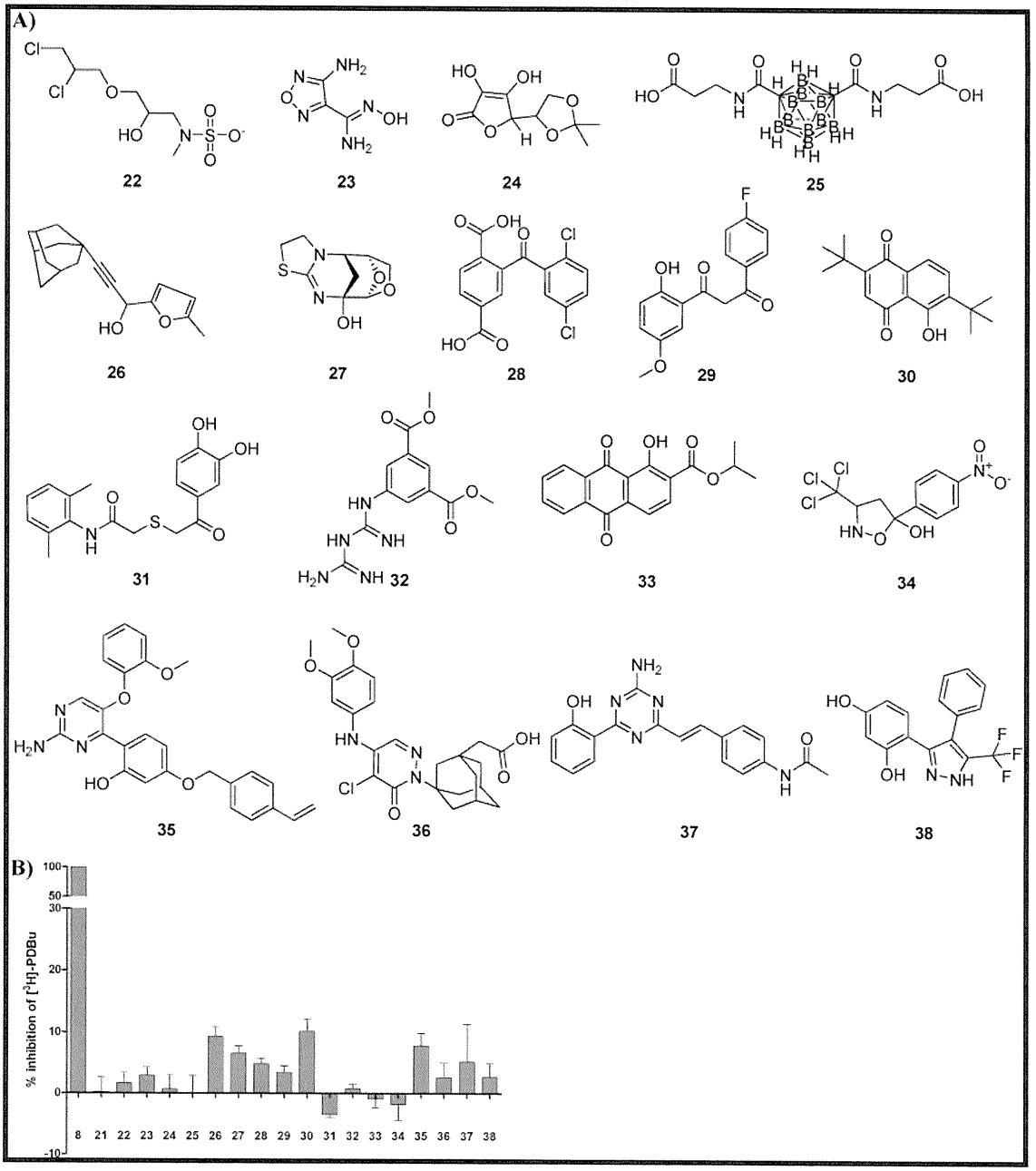

Figure 7. The RI competition assay of positive hit compounds found in fluorescent screening utilizing compound **1**. (A) Structures of test compounds obtained from screening. (B) Results of the inhibition assay based on RI methods. The concentration of compounds was fixed at 10 μM. The *X* axis indicates compound numbers. Columns show average inhibition obtained from triplicated experiments. Bars indicate standard errors.

In view of the above results, the present fluorescence-based evaluation of binding to the δC1b domain on microplates was deemed to be a promising alternative for the classical RI assay.

Expansion of the Fluorescence Evaluation to Screening of Library Compounds. As a proof-of-concept study, compound **1** was utilized in screening of a chemical library, supplied by the Screening Center at the Tokyo Medical and Dental University Screening Center. The structures of the library compounds were analyzed in advance of screening. For binding to the δC1b domain, pharmacophores including the carbonyl and hydroxy groups are necessary and only compounds including these functional groups were chosen. In the analysis of the library on microplates, compounds with more than 20% decrease of fluorescent intensity determined by triplicated assays were selected as candidates for further study. Compounds **22**−**38** were found from 2560 library compounds (Figure 7A) as candidate δC1b ligands. To further assess the binding affinity of these compounds, evaluation of binding by competition with the [^{3}H]PDBu was performed at a fixed concentration (10 μM) (Figure 7B). In this analysis, compounds **30** and **26**, with inhibition percentages at 10 μM of 10.2% and of 9.4%, respectively, showed the most and the second most potent binding affinities for the δC1b domain. The binding affinities of these compounds are still very low compared to that of DAG-lactones, but an SAR study of these compounds could lead to novel structure templates for synthetic PKC ligands. This analysis also revealed that compounds **24**, **25**, **31**, **32**, **33**, and **34** are false positive hits. The results obtained indicate that our screening system with a fluorescent

dx.doi.org/10.1021/bc100567k |*Bioconjugate Chem.* 2011, 22, 923–930

DAG-lactone derivative could be utilized for discovery of novel chemical leads for PKCδ.

CONCLUSION

A fluorescence-based method for chemical library screening has been developed. This method, which requires no washing steps, provides a linear response in relative binding affinity between compounds and is compatible with the classical RI assay for PKC ligands. By screening of more than 2500 library compounds, the method was proven to be a reliable means of discovery of compounds that bind to the C1b domain of PKCδ. The method would provide potent lead compounds that bind to the isozyme utilized in the assay. By utilization of the difference of the binding affinity of reporter compounds to different isozymes, it is possible that this screening system can provide an efficient selection of lead compounds highly specific to a target isozyme. This fluorescence-quenching method should be applicable to other known receptor−ligand combinations.

ASSOCIATED CONTENT

Supporting Information. Synthesis procedures and NMR, HRMS, and IR data. This material is available free of charge via the Internet at http://pubs.acs.org.

AUTHOR INFORMATION

Corresponding Author

*E-mail: tamamura.mr@tmd.ac.jp. Phone: +81-3-5280-8036. Fax: +81-3-5280-8039.

ACKNOWLEDGMENT

The authors thank Professor Masatoshi Hagiwara and Dr. Yukiko Okuno (Chemical Biology Screening Center, Tokyo Medical and Dental University) for their support in chemical library screening. This work was supported in part by Naito Foundation (W.N.) and Research Award of Graduate School of Biomedical Science, Tokyo Medical and Dental University (W.N. and T.I.)

REFERENCES

(1) Loving, G. S., Sainlos, M., and Imperiali, B. (2010) Monitoring protein interactions and dynamics with solvatochromic fluorophores. *Trends Biotechnol. 28*, 73–83.

(2) Rothman, D. M., Shults, M. D., and Imperiali, B. (2005) Chemical approaches for investigating phosphorylation in signal transduction networks. *Trends Cell Biol. 15*, 502–510.

(3) Terai, T., and Nagano, T. (2008) Fluorescent probes for bioimaging applications. *Curr. Opin. Chem. Biol. 12*, 515–521.

(4) Reymond, J. -L. (2008) Substrate arrays for fluorescence-based enzyme fingerprinting and high-throughput screening. *Ann. N.Y. Acad. Sci. 1130*, 12–20.

(5) Nomura, W., Tanabe, Y., Tsutsumi, H., Tanaka, T., Ohba, K., Yamamoto, N., and Tamamura, H. (2008) Fluorophore labeling enables imaging and evaluation of specific CXCR4−ligand interaction at the cell membrane for fluorescence-based screening. *Bioconjugate Chem. 19*, 1917–1920.

(6) Hayashida, O., Ogawa, N., and Uchiyama, M. (2007) Surface recognition and fluorescence sensing of histone by dansyl-appended cyclophane-based resorcinarene trimer. *J. Am. Chem. Soc. 129*, 13698–13705.

(7) Tsutsumi, H., Nomura, W., Abe, S., Mino, T., Masuda, A., Ohashi, N., Tanaka, T., Ohba, K., Yamamoto, N., Akiyoshi, K., and Tamamura, H. (2009) Fluorogenically active leucine zipper peptides as tag-probe pairs for protein imaging in living cells. *Angew. Chem., Int. Ed. 48*, 9164–9166.

(8) Nishizuka, Y. (1992) Intracellular signaling by hydrolysis of phospholipids and activation of protein kinase C. *Sceince 258*, 607–614.

(9) Newton, A. C. (1995) Protein kinase C: structure, function, and regulation. *J. Biol. Chem. 270*, 28495–28498.

(10) Watanabe, T., Ono, Y., Taniyama, Y., Hazama, K., Igarashi, K., Ogita, K., Kikkawa, U., and Nishizuka, Y. (1992) Cell division arrest induced by phorbol ester in CHO cells overexpressing protein kinase C-delta subspecies. *Proc. Natl. Acad. Sci. U.S.A. 89*, 10159–10163.

(11) Mischak, H., Pierce, J. H., Goodnight, J., Kazanietz, M. G., Blumberg, P. M., and Mushinski, J. F. (1993) Phorbol ester-induced myeloid differentiation is mediated by protein kinase C-alpha and -delta and not by protein kinase C-beta II, -epsilon, -zeta, and -eta. *J. Biol. Chem. 268*, 20110–20115.

(12) Li, C., Wernig, F., Leitges, M., Hu, Y., and Xu, Q. (2003) Mechanical stress-activated PKCdelta regulates smooth muscle cell migration. *FASEB J. 17*, 2106–2108.

(13) Ghayur, T., Hugunin, M., Talanian, R. V., Ratnofsky, S., Quinlan, C., Emoto, Y., Pandey, P., Datta, R., Huang, Y., Kharbanda, S., Allen, H., Kamen, R., Wong, W., and Kufe, D. (1996) Proteolytic activation of protein kinase C delta by an ICE/CED 3-like protease induces characteristics of apoptosis. *J. Exp. Med. 184*, 2399–2404.

(14) Alkon, D. L., Sun, M.-K., and Nelson, T. J. (2007) PKC signaling deficits: a mechanistic hypothesis for the origins of Alzheimer's disease. *Trends Pharmacol. Sci. 28*, 51–60.

(15) Wang, Q. J. (2006) PKD at the crossroads of DAG and PKC signaling. *Trends Pharmacol. Sci. 27*, 317–323.

(16) Marquez, V. E., and Blumberg, P. M. (2003) Synthetic diacylglycerols (DAG) and DAG-lactones as activators of protein kinase C (PK-C). *Acc. Chem. Res. 36*, 434–443.

(17) Nacro, K., Bienfait, B., Lee, J., Han, K.-C., Kang, J.-H., Benzaria, S., Lewin, N. E., Bhattacharyya, D. K., Blumberg, P. M., and Marquez, V. E. (2000) Conformationally constrained analogues of diacylglycerol (DAG). 16. How much structural complexity is necessary for recognition and high binding affinity to protein kinase C?. *J. Med. Chem. 43*, 921–944.

(18) Tamamura, H., Bienfait, B., Nacro, K., Lewin, N. E., Blumberg, P. M., and Marquez, V. E. (2000) Conformationally constrained analogues of diacylglycerol (DAG). 17. Contrast between *sn*-1 and *sn*-2 DAG lactones in binding to protein kinase C. *J. Med. Chem. 43*, 3209–3217.

(19) Tamamura, H., Sigano, D. M., Lewin, N. E., Blumberg, P. M., and Marquez, V. E. (2004) Conformationally constrained analogues of diacylglycerol. 20. The search for an elusive binding site on protein kinase C through relocation of the carbonyl pharmacophore along the *sn*-1 side chain of 1,2-diacylglycerol lactones. *J. Med. Chem. 47*, 644–655.

(20) Baba, Y., Ogoshi, Y., Hirai, G., Yanagisawa, T., Nagamatsu, K., Mayumi, S., Hashimoto, Y., and Sodeoka, M. (2004) Design, synthesis, and structure−activity relationship of new isobenzofuranone ligands of protein kinase C. *Bioorg. Med. Chem. Lett. 14*, 2963–2967.

(21) Baba, Y., Mayumi, S., Hirai, G., Kawasaki, H., Ogoshi, Y., Yanagisawa, T., Hashimoto, Y., and Sodeoka, M. (2004) Evaluation of series of isobenzofuranone dimers as PKCalpha ligands: implication for the distance between the two ligand binding sites. *Bioorg. Med. Chem. Lett. 14*, 2969–2972.

(22) Yanagita, R. C., Nakagawa, Y., Yamanaka, N., Kashiwagi, K., Saito, N., and Irie, K. (2008) Synthesis, conformational analysis, and biological evaluation of 1-hexylindolactam-V10 as a selective activator for novel protein kinase C isozymes. *J. Med. Chem. 51*, 46–56.

(23) Nakagawa, Y., Yanagita, R. C., Hamada, N., Murakami, A., Takahashi, H., Saito, N., Nagai, H., and Irie, K. (2009) A simple analogue of tumor-promoting aplysiatoxin is an antineoplastic agent rather than a tumor promoter: development of a synthetically accessible protein kinase C activator with bryostatin-like activity. *J. Am. Chem. Soc. 131*, 7573–7579.

(24) Martin, S. F., Josey, J. A., Wong, Y.-L., and Dean, D. W. (1994) General method for the synthesis of phospholipid derivatives of 1,2-*O*-diacyl-*sn*-glycerols. *J. Org. Chem. 59*, 4805–4820.

(25) Malolanarasimhan, K., Kedei, N., Sigano, D. M., Kelley, J. A., Lai, C. C., Lewin, N. E., Surawski, R. J., Pavlyukovets, V. A., Garfield, S. H., Wincovitch, S., Blumberg, P. M., and Marquez, V. E. (2007) Conformationally constrained analogues of diacylglycerol (DAG). 27. Modulation of membrane translocation of protein kinase C (PKC) isozymes alpha and delta by diacylglycerol lactones (DAG-lactones) containing rigid-rod acyl groups. *J. Med. Chem. 50*, 962–978.

(26) Nomura, W., Narumi, T., Ohashi, N., Serizawa, Y., Lewin, N. E., Blumberg, P. M., Furuta, T., and Tamamura, H. (2011) Synthetic caged DAG-lactones for photochemically-controlled activation of protein kinase C. *ChemBioChem 12*, 535–539.

(27) Mischak, H., Bodenteich, A., Kolch, W., Goodnight, J., Hofer, F., and Mushinski, J. F. (1991) Mouse protein kinase C-delta, the major isoform expressed in mouse hemopoietic cells: sequence of the cDNA, expression patterns, and characterization of the protein. *Biochemistry 30*, 7925–7931.

(28) Kazanietz, M. G., Krausz, K. W., and Blumberg, P. M. (1992) Differential irreversible insertion of protein kinase C into phospholipid vesicles by phorbol esters and related activators. *J. Biol. Chem. 267*, 20878–20886.

(29) List, B., Barbas, C. F., III, and Lerner, R. A. (1998) Aldol sensors for the rapid generation of tunable fluorescence by antibody catalysis. *Proc. Natl. Acad. Sci. U.S.A. 95*, 15351–15355.

(30) Davis, G. A. (1972) Dansylglycine as a fluorescent probe for aqueous solutions of cationic detergents. *J. Am. Chem. Soc. 94*, 5089–5090.

(31) Morii, T., Sugimoto, K., Makino, K., Otsuka, M., Imoto, K., and Mori, Y. (2002) A new fluorescent biosensor for inositol trisphosphate. *J. Am. Chem. Soc. 124*, 1138–1139.

(32) Matlock, D. L., and Heyduk, T. (1999) A real-time fluorescence method to monitor the melting of duplex DNA during transcription initiation by RNA polymerase. *Anal. Biochem. 270*, 140–147.

(33) Kakio, A., Nishimoto, S., Yanagisawa, K., Kozutsumi, Y., and Matsuzaki, K. (2001) Cholesterol-dependent formation of GM1 ganglioside-bound amyloid beta-protein, an endogenous seed for Alzheimer amyloid. *J. Biol. Chem. 276*, 24985–24990.

(34) Timofeevski, S. L., Prusakiewicz, J. J., Rouzer, C. A., and Marnett, L. J. (2002) Isoform-selective interaction of cyclooxygenase-2 with indomethacin amides studied by real-time fluorescence, inhibition kinetics, and site-directed mutagenesis. *Biochemistry 41*, 9654–9662.

(35) Sakamoto, S., and Kudo, K. (2008) Supramolecular control of split-GFP reassembly by conjugation of beta-cyclodextrin and coumarin units. *J. Am. Chem. Soc. 130*, 9574–9582.

(36) Sharkey, N. A., and Blumberg, P. M. (1985) Highly lipophilic phorbol esters as inhibitors of specific [^{3}H]phorbol 12,13-dibutyrate binding. *Cancer Res. 45*, 19–24.

(37) Ohashi, N., Nomura, W., Kato, M., Narumi, T., Lewin, N. E., Blumberg, P. M., and Tamamura, H. (2009) Synthesis of protein kinase Cdelta C1b domain by native chemical ligation methodology and characterization of its folding and ligand binding. *J. Pept. Sci. 15*, 642–646.

DOI: 10.1002/cmdc.201100542

A Synthetic C34 Trimer of HIV-1 gp41 Shows Significant Increase in Inhibition Potency

Wataru Nomura,[a] Chie Hashimoto,[a] Aki Ohya,[a] Kosuke Miyauchi,[b] Emiko Urano,[b] Tomohiro Tanaka,[a] Tetsuo Narumi,[a] Toru Nakahara,[a] Jun A. Komano,[b] Naoki Yamamoto,[c] and Hirokazu Tamamura*[a]

The development of new anti-HIV-1 drugs such as inhibitors of protease and integrase has been contributed to highly active anti-retroviral therapy (HAART) for the treatment of AIDS.[1] The entry of human immunodeficiency virus type 1 (HIV-1) into target cells is mediated by its envelope glycoprotein (Env), a type I transmembrane protein that consists of surface subunit gp120 and noncovalently associated transmembrane subunit gp41.[2] Sequential binding of HIV-1 gp120 to its cell receptor CD4 and a co-receptor (CCR5 or CXCR4) can trigger a series of conformational rearrangements in gp41 to mediate fusion between viral and cellular membranes.[3–5] The protein gp41 is hidden beneath gp120, and its ectodomain contains helical N- and C-terminal leucine/isoleucine heptad repeat domains, N-HR and C-HR. Particular regions of N-HR and C-HR are involved in membrane fusion, and 36-mer and 34-mer peptides, which are derived from N-HR and C-HR, have been designated as the N-terminal helix (N36) and C-terminal helix (C34), respectively. In the membrane fusion of HIV-1, these helices assemble to form a six-helical bundle (6-HB) consisting of a central parallel trimer of N36 surrounded by C34 in an antiparallel hairpin fashion. Synthetic peptides derived from these helices have potent antiviral activity against both laboratory-adapted strains and primary isolates of HIV-1.[6–9] They inhibit the membrane fusion stage of HIV-1 infection in a dominant-negative manner by binding to the counterpart regions of gp41 (N-HR or C-HR), blocking formation of the viral gp41 core.

Several potent anti-HIV-1 peptides based on the C-HR region have been discovered,[7,8] and T20 was subsequently developed as the clinical anti-HIV-1 drug enfuvirtide (Roche/Trimeris).[8,10–13] It is a 36-mer peptide derived from the gp41 C-HR sequence and can bind to the N-HR to prevent formation of the 6-HB in a dominant-negative fashion.[10] T20 therapy has brought safety, potent antiretroviral activity, and immunological benefit to patients, but its clinical application is limited by the development of resistance. The C-terminal helix C34 is also a C-HR-derived peptide, and contains the amino acid residues required for docking into the hydrophobic pocket, termed the "deep pocket", of the trimer of the N-HR region. This peptide potently inhibits HIV-1 fusion in vitro.[14] To date, several gp41 mimetics, especially those of N36 regions, which assemble these helical peptides with branched peptide linkers, have been synthesized as antigens.[15–19]

Recently, by using a novel template with C3-symmetric linkers of equal length, we synthesized a three-helix bundle mimetic that corresponds to the trimeric form of N36.[20] The antisera obtained from mice immunized by the peptide antigen showed strong recognition against the N36 trimer peptide with structural preference. At the same time, the trimer peptide was also investigated as a fusion inhibitor. However, the trimer N36 showed only a threefold increase in inhibition of HIV-1 fusion relative to the N36 monomer.[20] In terms of N36 content, the trimer and monomer have nearly the same inhibitory potency. This phenomenon is consistent with the results from other studies.[21–23] The multimerization of the functional unit, such as synthetic ligands against receptors, show synergistic binding and strong binding activity. Thus, we hypothesized that our strategy using C3-symmetric linkers in the design of trimer mimics of gp41 could be applied to the C34 peptide, which shows significant inhibition potency in the monomeric form. In the present study, we designed and synthesized a novel three-helical bundle structure of the trimeric form of C34. This equivalent mimic of the trimeric form of C34 was evaluated as a novel form of fusion inhibitor.

The C-terminal region of gp41 is known to be an assembly site involving a trimeric coiled-coil conformation. In the design of the C34-derived peptides C34REG-thioester (Figure 1 A) and C34REG (Figure 1 B), the triplet repeat of arginine and glutamic acid (RERERE) was added to the C-terminal end of the C34 sequence (residues 628–661) to increase aqueous solubility, and for C34REG-thioester, a glycine thioester was fused to the C terminus. To form a triple helix corresponding precisely to the gp41 pre-fusion form, we designed the novel C3-symmetric template depicted in Figure 1 C. This designed template linker has three branches of equal length, a hydrophilic structure, and a ligation site for coupling with C34REG-thioester. The template was synthesized as shown in Scheme 1. This approach uses native chemical ligation for chemoselective coupling of unprotected C34REG-thioester with a three-armed cysteine scaffold to produce triC34e (Figure 2).[24,25]

Circular dichroism (CD) spectra of C34REG and triC34e are shown in Figure 3 A. The peptides were dissolved in 50 mM sodium phosphate buffer with 150 mM NaCl, pH 7.2. Both spectra display minima at ~200 nm, indicating that these peptides form random structures. We previously reported that the

[a] Dr. W. Nomura, C. Hashimoto, A. Ohya, Dr. T. Tanaka, Dr. T. Narumi, T. Nakahara, Prof. Dr. H. Tamamura
Institute of Biomaterials and Bioengineering
Tokyo Medical and Dental University
2-3-10 Kandasurugadai, Chiyoda-ku, Tokyo 101-0062 (Japan)
E-mail: tamamura.mr@tmd.ac.jp

[b] Dr. K. Miyauchi, Dr. E. Urano, Dr. J. A. Komano
AIDS Research Center, National Institute of Infectious Diseases
1-23-1 Toyama, Shinjuku-ku, Tokyo 162-8640 (Japan)

[c] Prof. Dr. N. Yamamoto
Department of Microbiology, Yong Loo Lin School of Medicine
National University of Singapore
5 Science Drive 2, Singapore 117597 (Singapore)

Supporting information for this article is available on the WWW under http://dx.doi.org/10.1002/cmdc.201100542.

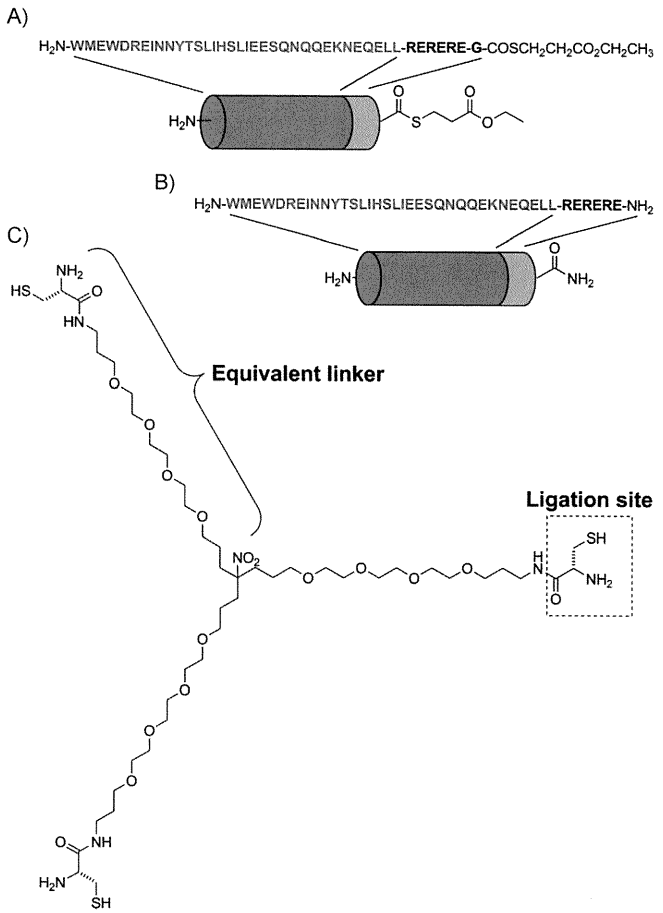

Figure 1. C34-derived peptides: A) C34REG-thioester and B) C34REG. C) The design of a C3-symmetric template.

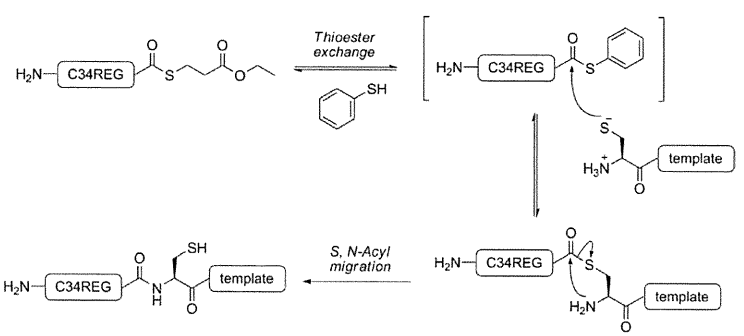

Figure 2. The native chemical ligation used for assembly of the C34REG-thioester on the template.

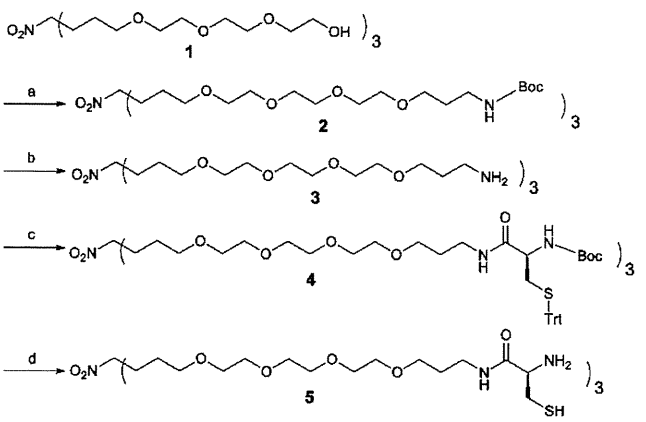

Scheme 1. Synthesis of the equivalently branched template **5**. *Reagents and conditions*: a) (3-bromopropyl)carbamic acid *tert*-butyl ester, NaH, THF; b) 4 M HCl/dioxane; c) Boc-Cys(Trt)-OH, EDCI·HCl, HOBt·H_2O, Et_3N, DMF; d) 90% aq. TFA.

helical content of the trimer triC34e and N36RE mixture is lower than that of the monomer C34REG and N36RE mixture. This is evidence that relative to the monomer C34REG, the trimer triC34e interacts with N36 only with difficulty, due to the assembly of three peptide strands by covalent bonds.

As the trimeric C34 was proven to interact with N36 helices, the potential HIV-1 inhibitory activities of the C-terminal peptides, C34REG and triC34e, were evaluated. The C34 peptide without the solubility-increasing sequence (3×[Arg-Glu], obtained from NIAID) was used as the monomeric control.[27] All peptides showed potent inhibitory activity in the viral fusion assay (Table 1), with the potency of triC34e being 100- and 40-fold higher than that of C34REG and C34 peptides, respectively. Notably, the triC34e trimer peptide is remarkably more potent in anti-HIV-1 activity than the monomer, indicating that a trimeric form is critical for inhibitory activity. Cytotoxicity from the peptides was not observed at concentrations of 15 μM for C34REG and C34, and 5 μM for triC34e.

We next carried out an assay for the inhibition of viral replication. As shown in Table 2, triC34e showed 30- and 20-fold higher inhibitory activity than peptides C34 and C34REG, respectively. In the two anti-HIV-1 assays, triC34e showed a great enhancement of activity over the C34 monomers. The IC_{50} values obtained in the assays are different, and this can be

N36 monomer N36RE and the N36 trimer triN36e form a highly structured α helix, and that the helical content of triN36e was greater than that of N36RE.[20,26] These results suggest that in contrast to N36-derived peptides, C34-derived peptides tend to form random structures both in the monomeric and trimeric forms. To assess the interaction of triC34e with N36, CD spectra of a mixture of triC34e with an N36-derived peptide, N36RE, were measured (Figure 3 B). The spectrum of the C34REG and N36RE mixture and that of the triC34e and N36RE mixture showed double minima at λ 208 and 222 nm, indicating that the peptide mixture forms an α-helical structure and that the

Table 1. IC_{50} and CC_{50} values determined by viral fusion inhibition and cell viability assays.

	C34 peptide[a]	C34REG	triC34e
IC_{50} [μM][b]	0.044	0.12	0.0013
CC_{50} [μM][c]	>15	>15	>5

[a] HIV-1 IIIB C34 peptide. [b] IC_{50} values are based on luciferase signals in TZM-bl cells infected with HIV-1 (NL4-3 strain). [c] CC_{50} values are based on the decrease in viability of TZM-bl cells. All data are the mean values from at least three experiments.

